European Journal of Control 79 (2024) 101023

Contents lists available at ScienceDirect

European Journal of Control

journal homepage: www.sciencedirect.com/journal/european-journal-of-control

A convex and robust distributed model predictive control for heterogeneous vehicle platoons

Hao Sun [a,*], Li Dai [b], Giuseppe Fedele [c], Boli Chen [a]

[a] Department of Electronic and Electrical Engineering, University College London, London, WC1E 6BT, UK
[b] School of Automation, Beijing Institute of Technology, Beijing, 100081, China
[c] Department of Informatics, Modelling, Electronics and Systems Engineering, University of Calabria, Rende, 87036, Italy

ARTICLE INFO

Recommended by T Parisini

Keywords:
Connected and autonomous vehicle
Distributed model predicted control
Convex optimization
Robust control

ABSTRACT

The roll out of connected and autonomous vehicle (CAV) technologies can be beneficial for road traffic in terms of road safety, traffic and energy efficiency. This paper addresses the platooning problem of heterogeneous CAVs with consideration of a time-varying leader speed and multi-dimensional uncertainties that include modeling uncertainties and local measurement disturbances. Resorting to a spatial domain modeling approach with appropriate coordination changes and the relaxation of nonconvex constraints, the traditional nonlinear optimal control problem formulation is convexified for improved computational efficiency and ease of implementation. Then, a convex and tube-based distributed model predictive control algorithm (DMPC) utilizing a predecessor-following communication topology is designed with certified theoretical properties, which can be boiled down to DMPC parameter tuning criteria. Finally, numerical results and comparisons against nominal and nonlinear DMPC-based methods are carried out to verify the performance and computational efficiency of the proposed method under different driving scenarios.

1. Introduction

With the advance of robotics, control and communication technology, connected and autonomous vehicles (CAVs) are predicted to improve road safety, transportation efficiency and energy consumption. One of the key applications of CAV technologies is vehicle platoon control. By exploiting inter-vehicular communication, cooperative controllers make CAVs move at the same speed and a small headway between consecutive vehicles to form a platoon. The work on vehicle platoon control can be dated back to the 1980s (Kanafani & Parsons, 1989; Shladover et al., 1991). Since then, many research organizations and automotive industries successively developed relative projects (Karafyllis, Theodosis, & Papageorgiou, 2023; Robinson, Chan, & Coelingh, 2010; Tsugawa, 2013).

There is rich literature dealing with platoon formation control, including consensus control (Karafyllis et al., 2023; Lunze, 2019), optimal control (Wang et al., 2020; Zhu, Zhao, & Zhong, 2019), data-driven control (Guo, Guo, Liu, Cao, & Chen, 2022; Lan, Zhao, & Tian, 2021), $\mathcal{H}$-infinity control (Liu, Xu, Cai, Yin, & Yan, 2023; Liu, Yao, Wang, & Lu, 2022; Wang et al., 2023; Xu et al., 2022), sliding mode control (Boo & Chwa, 2023; Zhou et al., 2022a) and model predictive control (MPC) (An & Talebpour, 2023; Huang, Chu, Wu, & He, 2019; Ozkan & Ma, 2022; Yu et al., 2016). In particular, MPC-based platooning schemes turn out to be one of the most preferable control solutions for their capability of handling the control and state constraints, which are ubiquitous in the vehicle platoons, such as powertrain limits, collision avoidance constraints and traffic regulation constraints. On the other hand, due to the technological advancement in inter-vehicular communication, distributed model predictive control (DMPC) solutions are receiving considerable research interest. They permit each controller to be deployed locally on each vehicle so that the computational efficiency and overall system resilience can be significantly improved as compared to centralized approaches (Feng et al., 2019; Gungor & Al-Qadi, 2020; Li, Bian, Li, Xu, & Wang, 2020; Wang et al., 2021; Zheng, Li, Li, Borrelli, & Hedrick, 2016). The inter-vehicle communication graph plays an important role in the DMPC platoon control design. A common assumption invoked to ensure the internal stability properties of a DMPC is the existence of a spanning tree within the platoon communication graph. Under such an assumption, a typical class of DMPC algorithm is proposed in Zheng et al. (2016), which discusses the conditions ensuring asymptotic stability of vehicle platooning with respect to several common communication topologies, such as predecessor-following (PF), predecessor-leader following (PLF)

* Corresponding author.
E-mail address: h.sun.20@ucl.ac.uk (H. Sun).
URL: https://profiles.ucl.ac.uk/81021-hao-sun (H. Sun).

https://doi.org/10.1016/j.ejcon.2024.101023
Received 19 November 2023; Received in revised form 24 April 2024; Accepted 28 May 2024
Available online 4 June 2024

Nomenclature

CAV	Connected and Autonomous Vehicle
(D)MPC	(Distributed) Model Predictive Control
ISS	Input-to-State Stability
PF	Predecessor-Following
PLF	Predecessor-Leader Following
TPLF	Two Predecessor-Leader Following
C_d, C_f	Air drag and rolling resistance coefficients
d, w	Modeling uncertainty and measurement noise
E, Δt	Kinetic energy and time headway of vehicle
g	Gravitational constant
m	Vehicle mass
r	Vehicle tire radius
T, ξ	Input torque and virtual input
η	Vehicle drive ratio
θ	Road slope angle
$\mathcal{E}$, δ	Normalized kinetic energy and time headway of vehicle
$\mathcal{T}$, ζ	Normalized input torque and virtual input
x, u, y	Actual state, input and output
x^a, u^a	Assumed state and input
$\hat{x}$, $\hat{y}$	Estimated state and output
$\bar{x}$, $\bar{u}$	Nominal state and input
x^*, u^*	Optimal state and input

and K-predecessor-leader following, either directed or undirected. An alternative DMPC algorithm is introduced in Qiang, Dai, Chen, and Xia (2022), where a bidirectional PF communication mechanism is utilized to enhance the feasibility as compared to unidirectional PF during the initial phase when the target of the leader is not known to all followers. On the other hand, to ensure that external disturbances are not amplified when propagating along the vehicle string, string stability has been widely investigated and usually addressed by involving extra MPC terminal constraints (Feng et al., 2019; Seiler, Pant, & Hedrick, 2004). Moreover, in Liu, Kurt, and Ozguner (2019), the cooperative merge-and-split control problem of a vehicle platoon is addressed by a two-step DMPC algorithm, which guarantees collision-free properties in addition to flexible platooning operation. The joining and leaving of vehicles may yield a time-varying communication topology among vehicles, and this problem is studied in Li et al. (2020) by another DMPC algorithm. In order to optimize the fuel economy of heavy-duty vehicle platoons, Turri, Besselink, and Johansson (2017) deals with a two-layer control architecture, where the two layers are responsible for vehicle speed preview based on road topography and real-time velocity control of the platoon, respectively. The mixed platoon of CAVs and human-driven vehicles are investigated in Gong and Du (2018), where non-autonomous vehicles are modeled by a macroscopic car-following model. The DMPC algorithm deployed on each CAV is shown to be effective in maintaining platoon formation in such a nominal case. Considering an electric vehicle platoon, Pi et al. (2022) has proposed a DMPC-based energy-efficient control solution for optimal energy recovery braking force distribution and therefore maximized energy efficiency.

In practice, the platoon systems inevitably involve uncertainties due to model mismatches and external perturbations. Existing solution methods are usually based on $\mathcal{H}$-infinity control (Liu et al., 2023; Wang et al., 2023; Xu et al., 2022) and sliding model control (Boo & Chwa, 2023; Zhou et al., 2022a) methods, whereas there is still room for developing novel robust MPC-based heterogeneous platoon control strategies. Recently, in Luo, Nguyen, Fleming, and Zhang (2021), a tube-based DMPC algorithm has been proposed to address process noise. It has been shown that robustness can be guaranteed in the presence of a PLF communication graph. A similar tube-based DMPC algorithm is adopted in Feng, Song, Li, Zhang, and Li (2021) to cope with the prediction uncertainties introduced by the non-controllable human-driven vehicles in the context of a mixed autonomy vehicle platoon. Communication delays represent another source of system uncertainty as data transmission inevitably introduces time delays under practical conditions due to insufficient bandwidths, over-length platoons, radio interference, etc. In this regard, a robust DMPC approach using min–max optimization is designed in Zhou et al. (2022b), which is proven to be robust against communication delays.

Although distributed control architecture is beneficial for computational efficiency, existing CAVs are still struggling to deal with nonlinear programming in real-time due to the limited onboard computational resources. Early results consider only a highly simplified linear longitudinal dynamic system, which can substantially reduce the computation time, however, the accuracy of the control solution may not be sufficient due to the lack of consideration of vehicle heterogeneity (Li, Li, Rajamani, & Wang, 2011; Stankovic, Stanojevic, & Siljak, 2000). The recent work in Hu, Bhowmick, Arvin, Lanzon, and Lennox (2020) proposed a feedback linearization method to deliberately compensate the system nonlinearities so that linear DMPC can be used with reduced computational effort. Nevertheless, robustness cannot be guaranteed by the feedback linearization scheme as modeling uncertainties, such as variable drag coefficients and slops are ignored. Current literature in this area is still very limited and requires further study. It is therefore of great interest to study accurate but also computationally efficient algorithms for platooning.

The present paper expands the author's prior work in Sun, Dai, and Chen (2022) on the robust heterogeneous vehicle platoon control by considering a time-varying leader speed and proposes a convex and tubed-based DMPC platooning algorithm with superior optimization efficiency and certified theoretical properties. The proposed distributed control scheme is based on the PF communication protocol, which does not impose significant communication demand as compared to PLF in Luo et al. (2021) and the bidirectional topology in Qiang et al. (2022). Both process and measurement disturbances are considered to capture more realistic uncertainties in practice. The effectiveness of the proposed method and its advantages over the existing approaches are demonstrated by numerical simulations and comparisons. The contributions of the paper are summarized as follows:

- The traditional nonlinear vehicle platooning problem is reformulated by a spatial domain modeling approach with respect to vehicle kinetic energy and the time gap between adjacent vehicles. In this context, coupled state constraints for collision avoidance and platoon formation can be decoupled, such that feasibility and stability guarantees can be justified in a more handy way. Moreover, space-dependent coefficients, such as the rolling resistance and road slopes, can be accurately modeled.
- Following the last point, a convex optimization-based control framework is developed so that the optimal solution can be efficiently obtained at each step. Quantitative analysis in terms of computational efficiency is performed in the simulation section by numerical comparison with a traditional nonlinear DMPC approach. Moreover, the validity of the convex reformulation is rigorously analyzed.
- In contrast to the existing works that consider only partial disturbances in the platoon system, both unmodeled motion dynamics, and sensor measurement disturbances of the position and velocity are considered and addressed in this paper by a tube-based DMPC approach. The theoretical analysis reveals the DMPC parameter tuning criteria by which recursive feasibility and input-to-state stability (ISS) of the proposed algorithm can be guaranteed when the velocity of the leader vehicle reaches a steady state.

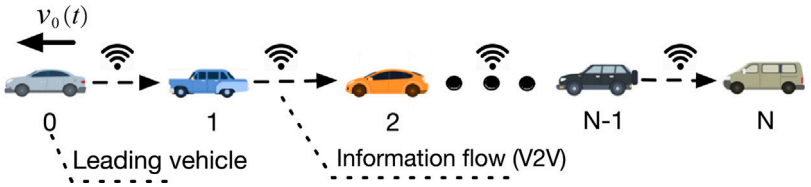

Fig. 1. A heterogeneous vehicle platoon with the PF communication protocol.

The remainder of this paper is organized as follows. The modeling framework and the communication topology are introduced in Section 2. In Section 3, the methodology of this distributed robust platoon control problem is proposed. In Section 4, theoretical analysis of recursive feasibility, Lyapunov asymptotic stability and auxiliary variable validation are demonstrated. Simulation results are presented in Section 5. Finally, Section 6 concludes this work.

Notation: Let $\mathbb{R}$, $\mathbb{R}_{\geq 0}$, $\mathbb{R}_{>0}$ denote the real, the non-negative real and the strict positive real sets of numbers, respectively. Given a vector $\mathbf{x} \in \mathbb{R}^n$, the Euclidean norm of $\mathbf{x}$ is denoted by $|\mathbf{x}|$. Given a time-varying vector $\mathbf{x}(t) \in \mathbb{R}^n$, $t \in \mathbb{R}_{\geq 0}$ we will denote as $\|\mathbf{x}\|_\infty$ the quantity $\|\mathbf{x}\|_\infty = \sup_{t\geq 0}|\mathbf{x}(t)|$. Given a matrix $\mathbf{A} \in \mathbb{R}^{n\times n}$, then $\|\mathbf{A}\|$ will denote $\max_{\mathbf{x}\in\mathbb{R}^n\setminus 0}\{|\mathbf{A}\mathbf{x}|/|\mathbf{x}|\}$, and $\mathbf{A}_{[i,j]}$ represent (i,j)th entry of the matrix. The Minkowski sum of sets $\mathbb{W}, \mathbb{V}$ is $\mathbb{W} \oplus \mathbb{V} = \{\ x + y \mid x \in \mathbb{W}, y \in \mathbb{V}\ \}$; the Minkowski difference of sets $\mathbb{W}, \mathbb{V}$ is $\mathbb{W} \ominus \mathbb{V} = \{\ x \mid x \oplus \mathbb{V} \subseteq \mathbb{W}\ \}$.

2. Problem statement

As shown in Fig. 1, this paper considers a vehicle platoon of $N+1$ heterogeneous CAVs. Without loss of generality, the leading CAV is indexed by 0 and the followers are indexed by $i \in \mathcal{N}$ with $\mathcal{N} = \{1, 2, \ldots, N\}$. Vehicle-to-vehicle (V2V) communication is enabled in the platoon and follows a unidirectional PF information flow topology by which each vehicle only receives information from the one immediately ahead. This communication protocol is commonly used in vehicle platooning due to its relatively lower data exchange demand compared to other topologies.

Next, we will first briefly review the nominal time-domain modeling framework of the platooning problem, and then a convex reformulation of the problem in the space domain will be introduced.

2.1. The nominal modeling framework in the time domain

The longitudinal dynamics of each following vehicle are described as:

$$\dot{s}_i(t) = v_i(t), \tag{1a}$$

$$\dot{v}_i(t) = \frac{1}{m_i}\left(\frac{\eta_i}{r_i}T_i(t) - C_{d,i}v_i^2(t) - m_i g C_{s,i}(t)\right),\ i \in \mathcal{N} \tag{1b}$$

where $s_i(t)$ is the position of vehicle i, $v_i(t)$ is the velocity, vehicle mass is denoted by m_i, g is the gravity constant, η_i is the final drive ratio, r_i is the tire radius, $C_{d,i}$ is the aerodynamic drag coefficient, and $T_i(t)$ is the driving/braking torque, acting as the control input of the follower. Moreover, $C_{s,i}(t)$ is the synthetic coefficient of the tire friction and gradient forces

$$C_{s,i}(t) = C_{f_i}\cos\theta_i(t) + \sin\theta_i(t), i \in \mathcal{N} \tag{2}$$

with C_{f_i} the rolling resistance coefficient and $\theta_i(t)$ the road slope angle.

The common objective of platoon control in the noise-free scenario requires all following vehicles to move at the same speed as the leading vehicle while following the constant time-headway policy between adjacent vehicles (Karafyllis et al., 2023; Lunze, 2019):

$$\lim_{t\to\infty}\|v_i(t) - v_0(t)\| = 0, \tag{3a}$$

$$\lim_{t\to\infty}\|s_i(t) - s_{i-1}(t) - h(t)\| = 0,\ \forall i \in \mathcal{N} \tag{3b}$$

where $v_0(t) \in [v_{\min}, v_{\max}]$ is the target speed of the leading vehicle, $h(t)$ is the desired spacing, proportional to speed $v_0(t)$. To complete the framework, the following constraints are also required for safety purposes and for the fulfillment of control limits

$$v_{\min} \leq v_i(t) \leq v_{\max}, \tag{4a}$$

$$h_{\min} \leq s_i(t) - s_{i-1}(t) \leq h_{\max}, \tag{4b}$$

$$T_{i,\min} \leq T_i(t) \leq T_{i,\max},\ \forall i \in \mathcal{N} \tag{4c}$$

in which $\{v_{\min}, v_{\max}\}$, $\{h_{\min}, h_{\max}\}$ (proportional to $v_{\min}$ and $v_{\max}$, respectively) and $\{T_{i,\min}, T_{i,\max}\}$ represent minimum and maximum limits for the driving speed, headway distance, and individual torque, respectively. As it can be noticed, the speed and headway distance limits are subject to driving conditions (*e.g.*, highway, rural, etc.), thus identical for all vehicles.

2.2. A convex modeling approach

Instead of the commonly used time-domain modeling approach with respect to the position and velocity of individual vehicles, as given in (1)–(4), this paper proposes to use a novel space domain modeling approach with state transformation to reformulate the platooning system, which (1) permits the control problem to be formulated as a convex optimization problem for rapid solution search, and (2) facilitates the design of the DMPC algorithm, as will be elaborated later.

Consider s the independent variable of traveled space (waypoint on the line of travel). The transformation from time to space domain is accomplished by replacing the independent variable t with s via

$$\frac{d}{ds} = \frac{1}{v}\frac{d}{dt}.$$

Let $E_i(s) = \frac{1}{2}m_i v_i^2(s)$ and $\Delta t_i(s) = t_i(s) - t_{i-1}(s), \forall i \in \mathcal{N}$ denote the kinetic energy of vehicle i and its time headway with respect to the preceding $(i-1)$-th vehicle, respectively. In view of (1), the dynamics of both variables in the space domain are governed by the following differential equations:

$$\frac{d}{ds}\Delta t_i(s) = \frac{1}{\sqrt{2E_i(s)/m_i}} - \frac{1}{\sqrt{2E_{i-1}(s)/m_{i-1}}}, \tag{5a}$$

$$\frac{d}{ds}E_i(s) = \frac{\eta_i}{r_i}T_i(s) - 2\frac{C_{d,i}}{m_i}E_i(s) - m_i g C_{s,i}(s). \tag{5b}$$

where $E_i(s) > 0, \forall s$ to avoid the singularity and it can be enforced by (7a) with $v_{\min} \geq 0$. As a consequence, the nominal objectives (3) and the constraints (4) can be replaced by:

$$\lim_{s\to\infty}\|E_i(s) - \frac{1}{2}m_i v_0^2(s)\| = 0 \tag{6a}$$

$$\lim_{s\to\infty}\|\Delta t_i(s) - \Delta_0\| = 0,\ \forall i \in \mathcal{N} \tag{6b}$$

and

$$E_{i,\min} \leq E_i(s) \leq E_{i,\max}, \tag{7a}$$

$$\Delta t_{\min} \leq \Delta t_i(s) \leq \Delta t_{\max}, \tag{7b}$$

$$T_{i,\min} \leq T_i(s) \leq T_{i,\max},\ \forall i \in \mathcal{N} \tag{7c}$$

where $E_{i,\min} = \frac{1}{2}m_i v_{\min}^2$ and $E_{i,\max} = \frac{1}{2}m_i v_{\max}^2$, Δ_0 is the desired time headway between consecutive vehicles. Note that $v_{\min}$ in the space

domain formulation can only be set to a non-zero constant to prevent singularity issues in (5a).[1] Being $E_i(s) > 0$, (6a) is equivalent to (3a). The time headway target (6b) and the constraint (7b) are surrogates of the headway distance objective and constraint given in (3b) and (4b) with $\Delta t_{\min}$ and $\Delta t_{\max}$ the minimum and maximum time headway, respectively. By substituting the coupled state constraints (4b) with the state constraint (7b), the uncertainties involved in the information received from the preceding vehicle can be immediately taken into consideration as the modeling error in (5a).

Now, we have all ingredients to formulate the distributed control problem for CAV i in the space domain.

OCP 1.

$$\min_{T_i} \quad J_i(\Delta t_i, E_i, T_i) \tag{8a}$$

$$\text{s.t. : (5), (7)} \tag{8b}$$

where the cost function $J_i(\Delta t_i, E_i, T_i)$ related to the quadratic control objectives (6), will be designed later in Section 3.2. It is noteworthy that OCP 1 is a non-convex programming problem because of the nonlinear dynamics in (5a). In order to improve the computational efficiency, a convex reformulation of (5a) is utilized:

$$\frac{d}{ds}\Delta t_i(s) = \xi_i(s) - \frac{1}{v_{i-1}(s)} \tag{9a}$$

$$\xi_i(s) \geq \frac{1}{\sqrt{2E_i(s)/m_i}},\ i \in \mathcal{N} \tag{9b}$$

where $\xi_i(s)$ is a fictitious control input used in place of the nonlinear term $\frac{1}{\sqrt{2E_i(s)/m_i}}$ that depends on the local state $E_i(s)$. As such, the nonlinear differential constraint (5a) can be relaxed to a combination of linear differential equations and a convex constraint in an optimal control problem. Consequently, OCP 1 can be convexified, leading to

OCP 2.

$$\min_{T_i, \xi_i} \quad J_i(\Delta t_i, E_i, T_i) \tag{10a}$$

$$\text{s.t. : (5b), (7), (9)} \tag{10b}$$

It is worth noting that the validity of the solution of OCP 2 relies on the tightness of (9b), which is addressed later by Proposition 1 in Section 4.

3. Tube-based distributed model predictive control

The main algorithm is introduced in this section. In the first place, the reformatted system equations are introduced. Based on that, the tube-based MPC algorithm is inherited from the theoretical framework proposed in Mayne, Raković, Findeisen, and Allgöwer (2006), then the local MPC problem is formulated for each following vehicle under a distributed control mechanism.

3.1. Tube-based MPC

For the sake of introducing the MPC-based algorithm and taking into account system uncertainties, such as modeling error and measurement noise, in a unified framework, the system differential Eqs. (5b) and (9a) are discretized and rewritten in a normalized form as follows:

$$\begin{aligned} x_i(k+1) &= A_i x_i(k) + B_i u_i(k) + \gamma_i(k) + d_i(k) \\ y_i(k) &= C x_i(k) + w_i(k), i \in \mathcal{N} \end{aligned} \tag{11}$$

[1] In the low driving speed scenario (*e.g.* urban driving), $v_{\min}$ can be set to a sufficiently small positive constant to avoid sacrificing the generality of the formulation.

$$A_i = \begin{bmatrix} 1 & 0 \\ 0 & 1 - \frac{2C_{d,i}}{m_i}\Delta s \end{bmatrix},\ B_i = \begin{bmatrix} \Delta s & 0 \\ 0 & \frac{\eta_i}{r_i}\Delta s \end{bmatrix},\ C = \begin{bmatrix} 1 & 0 \\ 0 & 1 \end{bmatrix},$$

$$\gamma_i(k) = \begin{bmatrix} -f_i\left(\hat{\mathcal{E}}_{i-1}(k)\right)\Delta s \\ -\frac{m_i g C_{s,i}(k)}{E_{\max}}\Delta s \end{bmatrix}$$

where $k = 0, 1, \ldots, \bar{k}$, $\Delta s \in \mathbb{R}_{>0}$ denotes the sampling distance interval and $\bar{k}\Delta s$ is the total length of the mission. The normalized state vector of Δt_i and E_i is defined as $x_i(k) \triangleq [\delta_i(k)\ \mathcal{E}_i(k)]^\top \in \mathbb{X}_i$ with $\delta_i(k) \triangleq \frac{\Delta t_i(k)}{\Delta t_{\max}}$, $\mathcal{E}_i(k) \triangleq \frac{E_i(k)}{E_{\max}}$ and $E_{\max} \triangleq \frac{1}{2}\bar{m}v_{\max}^2$, in which $\bar{m} \geq \max_{i\in\mathcal{N}} m_i$. Note that $\bar{m}$ can be conservatively designed without the global information about all vehicles' mass. Then, it holds that

$$\mathbb{X}_i \triangleq \left\{ x_i \mid \frac{\Delta t_{\min}}{\Delta t_{\max}} \leq \delta_i(k) \leq 1, \frac{E_{i,\min}}{E_{\max}} \leq \mathcal{E}_i(k) \leq 1 \right\}.$$

Similarly, the normalized input is denoted by $u_i \triangleq [\zeta_i(k)\ \mathcal{T}_i(k)]^\top \in \mathbb{U}_i$, where $\zeta_i(k) \triangleq \frac{\xi_i(k)}{\Delta t_{\max}}$, $\mathcal{T}_i(k) \triangleq \frac{T_i(k)}{E_{\max}}$ and $\mathbb{U}_i \triangleq \{u_i \mid \frac{T_{i,\min}}{E_{\max}} \leq \mathcal{T}_i(k) \leq \frac{T_{i,\max}}{E_{\max}}\}$. After the normalization, $\mathbb{X}_i \times \mathbb{U}_i$ involving (9b) becomes $\zeta_i(k) \geq f_i(\mathcal{E}_i(k))$, where the function $f_i(\cdot) : \mathbb{R}_{>0} \to \mathbb{R}_{>0}$ is defined as:

$$f_i(\mathcal{E}_i) \triangleq 1/(\Delta t_{\max}\sqrt{2E_{\max}\mathcal{E}_i/m_i}). \tag{12}$$

The normalized measurement y_i of δ_i and $\mathcal{E}_i$ obtained by the ith vehicle's onboard sensors (*e.g.*, front radar and speedometer). $\gamma_i(k)_{[1,1]}$ represents external information of the preceding vehicle $i-1$. In particular, $\hat{\mathcal{E}}_{i-1}(k)$ is an estimate of $\mathcal{E}_{i-1}(k)$ obtained and shared by the preceding vehicle $i-1$ at step $k-1$, which will be defined later on in Section 3.2. On the other hand, $\gamma_i(k)_{[2,1]}$ embodies the impact of the drag caused by road slope. Owing to the space domain model, space varying coefficient $C_{s,i}(k)$ can be easily incorporated to capture different road conditions, therefore enabling a less conservative disturbance bound in the robust control framework compared to the traditional time-domain scheme. Next, the system uncertainties are defined, $d_i(k) \in \mathbb{D}_i$ is the normalized modeling uncertainty and $w_i(k) \in \mathbb{W}_i$ represents the normalized measurement noise. Herein, $\mathbb{D}_i$ and $\mathbb{W}_i$ are two compact convex sets defined by $\mathbb{D}_i = \{d_i(k) \in \mathbb{R}^2 \mid \|d_i(k)\|_\infty \leq \overline{d}_i \in \mathbb{R}_{>0}\}$ and $\mathbb{W}_i = \{w_i(k) \in \mathbb{R}^2 \mid \|w_i(k)\|_\infty \leq \overline{w}_i \in \mathbb{R}_{>0}\}$. As it can be noticed, $d_i(k)$ accounts for the mismatch between the estimate $f_i\left(\hat{\mathcal{E}}_{i-1}(k)\right)\Delta s$ and $f_i\left(\mathcal{E}_{i-1}(k)\right)\Delta s$ that is constructed by the accurate information from the preceding vehicle (the only source of the disturbance appears in the dynamic equation of δ_i) as well as the unmodeled nonlinearities (*e.g.* headway-dependent air drag coefficients), while sensor measurement noises of the time headway and velocities are taken into account by w_i. Consider $\delta_0 \triangleq \Delta_0/\Delta t_{\max}$ the target gap and $\overline{m}_{i,0}\mathcal{E}_0(k)$ the target kinetic energy of vehicle i with $\overline{m}_{i,j} \triangleq m_i/m_j, j \neq i$. The control objective in the presence of uncertainties is defined by

$$\lim_{k\to\infty} \|x_i(k) - x_{i,des}^*\| = \sigma_i \tag{13}$$

where $x_{i,des}^* \triangleq [\delta_0\ \ \overline{m}_{i,0}\mathcal{E}_0]^\top$, and σ_i is an invariant set with respect to the system uncertainties. Note that $x_{i,des}^*$ is the target state of the platoon, involving the globally known target gap δ_0 and the velocity of the leading vehicle, which is initially unknown to the ith vehicle. Detailed discussion of this will be linked to the MPC design and the theoretical analysis given in Section 4.1.

The following assumption will be used throughout the paper.

Assumption 3.1. $f_i(\cdot), \forall i \in \mathcal{N}$ in the system Eq. (11) is Lipschitz in $\mathbb{X}_i$ with a constant κ_i.

Next, we define the nominal unperturbed system of (11), which will be instrumental for the tube-MPC design, introduced later on in this Section

$$\bar{x}_i(k+1) = A_i\bar{x}_i(k) + B_i\bar{u}_i(k) + \gamma_i(k) \tag{14a}$$

$$\bar{y}_i(k) = C\bar{x}_i(k) \tag{14b}$$

where $\bar{x}_i(k) \triangleq [\bar{\delta}_i(k)\ \bar{\mathcal{E}}_i(k)]^\top$ is the nominal state, $\bar{u}_i(k) \triangleq [\bar{\zeta}_i(k)\ \bar{\mathcal{T}}_i(k)]^\top$ is the nominal control input and $\bar{y}_i(k)$ is the nominal output.

By applying the Luenberger observer, the state of the actual system (11) can be estimated by:

$$\hat{x}_i(k+1) = A_i\hat{x}_i(k) + B_iu_i(k) + \gamma_i(k) + L_i(y_i(k) - \hat{y}_i(k))$$
$$\hat{y}_i(k) = C\hat{x}_i(k) \tag{15}$$

where L_i is the observer gain, designed individually for each vehicle, such that $A_i - L_iC$ is stable. Considering the state estimation error $\tilde{x}_i = x_i - \hat{x}_i$, its dynamics are governed by:

$$\tilde{x}_i(k+1) = (A_i - L_iC)\tilde{x}_i(k) + (d_i(k) - L_iw_i(k)) \tag{16}$$

In addition, the term $d_i(k) - L_iw_i(k)$ is bounded by a set $\tilde{\Omega}_i$, expressed as

$$\tilde{\Omega}_i \triangleq \mathbb{D}_i \oplus (-L_i\mathbb{W}_i) \tag{17}$$

Furthermore, the robust invariant set $\tilde{\mathbb{S}}_i$ of $\tilde{x}$ with respect to the process and measurement disturbances can be obtained by

$$\tilde{\mathbb{S}}_i = \oplus_{k=0}^{\infty}(A_i - L_iC)^k\tilde{\Omega}_i\,. \tag{18}$$

Consider $e_i(k) = \hat{x}_i(k) - \bar{x}_i(k)$ the mismatch between the observer state and the nominal system. Then the control law is constructed by

$$u_i(k) = \bar{u}_i(k) + K_ie_i(k) \tag{19}$$

where $\bar{u}_i(k)$ is determined by solving a nominal MPC problem subject to (14) and tightened state and input constraints, defined later on in (21), and K_i is the prespecified feedback control gain, which stabilizes $A_i + B_iK_i$. By applying (19) to (15), we obtain

$$\hat{x}_i(k+1) = A\hat{x}_i(k) + B_i\bar{u}_i(k) + B_iK_ie_i(k) + \gamma_i(k) + L_iC\tilde{x}_i(k) + L_iw_i(k)$$

In virtue of the nominal system (14), the dynamics of the tracking error $e_i(k)$ is given by

$$e_i(k+1) = (A_i + B_iK_i)e_i(k) + (L_iC\tilde{x}_i(k) + L_iw_i(k))$$

where the uncertainties term $L_iC\tilde{x}_i(k) + L_iw_i(k)$ is confined by

$$\overline{\Omega}_i \triangleq L_iC\tilde{\mathbb{S}}_i \oplus L_i\mathbb{W}_i.$$

Similar to (18), the robust invariant set $\tilde{\mathbb{S}}_i$ of e_i follows

$$\overline{\mathbb{S}}_i = \oplus_{k=0}^{\infty}(A_i + B_iK_i)^k\overline{\Omega}_i \tag{20}$$

According to Mayne et al. (2006), Vilaivannaporn, Boonsith, Pornputtapitak, and Bumroongsri (2021), to ensure the satisfaction of the original state and control constraints, $x_i(k) \in \mathbb{X}_i$ and $u_i(k) \in \mathbb{U}_i$, in the presence of the perturbations, tightened state and input constraints

$$\overline{x}_i \in \mathbb{X}_i \ominus (\tilde{\mathbb{S}}_i \oplus \overline{\mathbb{S}}_i), \qquad \overline{u}_i \in \mathbb{U}_i \ominus K_i\overline{\mathbb{S}}_i. \tag{21}$$

are enforced in place of the originals when solving the MPC problem (see (26) that will be introduced later in Section 3.2) In the following, for the sake of the brevity, we let

$$\bar{\mathbb{X}}_i \triangleq \mathbb{X}_i \ominus (\tilde{\mathbb{S}}_i \oplus \overline{\mathbb{S}}_i), \qquad \bar{\mathbb{U}}_i \triangleq \mathbb{U}_i \ominus K_i\overline{\mathbb{S}}_i \tag{22}$$

3.2. Distributed platoon control framework

Consider N_p the prediction horizon for each local MPC. To introduce the DMPC framework, let us define $x_i^*(j|k) \triangleq [\delta_i^*(j|k)\ \mathcal{E}_i^*(j|k)]^\top$ and $u_i^*(j|k) \triangleq [\zeta_i^*(j|k)\ \mathcal{T}_i^*(j|k)]^\top$ the optimal state and input trajectory, respectively. The optimal trajectories are obtained by iteratively solving each local MPC problem (see $\mathcal{P}_i(k)$ defined in (26)). In addition, define $x_i^a(j|k) \triangleq [\delta_i^a(j|k)\ \mathcal{E}_i^a(j|k)]^\top$ and $u_i^a(j|k) \triangleq [\zeta_i^a(j|k)\ \mathcal{T}_i^a(j|k)]^\top$ respectively the assumed state and control trajectory, which are shared with the neighboring vehicle by the PF communication. Finally, consider $x_{i,des}(j|k) \triangleq [\delta_0\ \mathcal{E}_{i,des}(j|k)]^\top$ the desired state trajectory. Specifically, $\mathcal{E}_{i,des}(j|k)$ is set to as $\mathcal{E}_{i,des}(j|k) = \overline{m}_{i,i-1}\mathcal{E}_{i-1}^a(j|k)$. The kth step assumed trajectories $(x_i^a(:\,|k), u_i^a(:\,|k))$ are constructed by using the $(k-1)$th step optimal solution as follows:

$$u_i^a(j|k) = u_i^*(j+1|k-1),\ \forall j \in \{0, 1, \dots, N_p - 2\} \tag{23}$$

which yields

$$x_i^a(j|k) = x_i^*(j+1|k-1),\ \forall j \in \{0, 1, \dots, N_p - 1\} \tag{24}$$

Moreover, $u_i^a(N_p-1|k)$ is designed to render

$$x_i^a(N_p|k) = A_ix_i^a(N_p-1|k) + B_iu_i^a(N_p-1|k) + \gamma_i(N_p-1|k) = x_{i,des}(N_p|k). \tag{25}$$

The existence of such a feasible $u_i^a(N_p-1|k)$ is characterized by Assumption 4.2 given in Section 4.1.

Considering the control objectives defined in (13), we formulate the local MPC problem $\mathcal{P}_i(k)$ for each vehicle $i \in \mathcal{N}$, at step k, as

$$\mathcal{P}_i(k):$$
$$\min_{\bar{u}_i}\ J_i(\bar{x}_i(:\,|k), \bar{u}_i(:\,|k), x_i^a(:\,|k), x_{i,des}(:\,|k))$$
$$= \sum_{j=0}^{N_p-1} l_i(\bar{x}_i(j|k), \bar{u}_i(j|k), x_i^a(j|k), x_{i,des}(j|k)) + \sum_{j=0}^{N_p-2}\psi_i|\bar{\zeta}_i(j|k) - f_i(\bar{\mathcal{E}}_i(j|k))| \tag{26a}$$

$$\textbf{s.t. for } j = 0, 1, 2, \dots, N_p - 1$$
$$\bar{x}_i(j+1|k) = A_i\bar{x}_i(j|k) + B_i\bar{u}_i(j|k) + \gamma_i(j|k) \tag{26b}$$
$$\bar{x}_i(j|k) \in \bar{\mathbb{X}}_i(k) \tag{26c}$$
$$\bar{u}_i(j|k) \in \bar{\mathbb{U}}_i \tag{26d}$$
$$(\bar{x}_i(j|k), \bar{u}_i(j|k)) \in \bar{\mathbb{X}}_i(k) \times \bar{\mathbb{U}}_i \tag{26e}$$
$$\bar{x}_i(0|k) = y_i(k) \tag{26f}$$
$$\bar{x}_i(N_p|k) \in \mathbb{X}_{f,i} \tag{26g}$$

where (26a) is the cost function that will be specified later in (31). (26b) represents the nominal system introduced in (14), where the estimate $\hat{\mathcal{E}}_{i-1}(j|k)$ in $\gamma_i(j|k)$ is defined by

$$\hat{\mathcal{E}}_{i-1}(j|k) = \begin{cases} \mathcal{E}_{i-1}^a(N_p|k), & \text{if } x_{i-1}^a(N_p|k) = x_{i-1}^a(N_p|k-1), \\ \mathcal{E}_{i-1}^a(j|k), & \text{if } x_{i-1}^a(N_p|k) \neq x_{i-1}^a(N_p|k-1), \end{cases} \quad \forall j \in \{0, 1, \dots, N_p\}\,. \tag{27}$$

As it can be noticed, $\hat{\mathcal{E}}_{i-1}(j|k)$ is frozen at $\mathcal{E}_{i-1}^a(N_p|k)$ if the terminal step of the preceding vehicle's assumed trajectory (*i.e.*, desired trajectory owing to (25)) remains the same for two consecutive steps, which usually happens when the leader vehicle reaches a steady state speed. Conversely, if $x_{i-1}^a(N_p|k) \neq x_{i-1}^a(N_p|k-1)$ (which implies $i-1$th vehicle's desired speed is time-varying), time-varying estimate $\hat{\mathcal{E}}_{i-1}(j|k)$ is employed to enable the ith vehicle to keep up with the preceding vehicle. The state and input constraints are taken into account by (26c), (26d) and (26e). Specifically, $\bar{\mathbb{X}}_i(k)$ in (26c) is defined by $\bar{\mathbb{X}}_i(k) = \bar{\mathbb{X}}_i \ominus \mathbb{H}_i(k)$, where $\mathbb{H}_i(k)$ is a set to further shrink the feasible set of the state to cope with the disturbances introduced at the initialization phase. It is designed as

$$\mathbb{H}_i(k) = (\bar{k} - k)\bar{\mathbb{H}}_i \tag{28}$$

where $\bar{\mathbb{H}}_i \triangleq \{(\varepsilon_1, \varepsilon_2) \in \mathbb{R}^2 \mid \varepsilon_1 \le \bar{w}_i + \bar{d}_i,\ \varepsilon_2 \le \bar{\varepsilon}\}$ with $\bar{\varepsilon} \triangleq (\bar{w}_i + \bar{d}_i) + N_p\kappa_i(\bar{w}_i + \bar{d}_i)\Delta s$. The feasible set of the control input, $\bar{\mathbb{U}}_i$, in (26d) is given in (22). In view of (9b), the coupled constraint (26e) represents

$$\bar{\mathbb{X}}_i(k) \times \bar{\mathbb{U}}_i \triangleq \{(\bar{\mathcal{E}}, \bar{\zeta}_i) \mid \bar{\zeta}_i(j|k) \ge f_i(\bar{\mathcal{E}}_i(j|k))\} \tag{29}$$

The initial and terminal constraints of the MPC are specified by (26f) and (26g), respectively. In particular, the terminal set $\mathbb{X}_{f,i}$ is defined as

$$\mathbb{X}_{f,i} \triangleq \{\bar{x}_i(N_p|k) \mid |\bar{\mathcal{E}}_i(N_p|k) - \overline{m}_{i,i-1}\mathcal{E}_{i-1}^a(N_p|k)| \le \bar{w}_i + \bar{d}_i,\ |\bar{\delta}_i(N_p|k) - \delta_0| \le \bar{\varepsilon}\} \tag{30}$$

which ensures the state trajectory enters a terminal set and $x_{i,des}(N_p|k) \in \mathbb{X}_{f,i} \subseteq \bar{\mathbb{X}}_i \ominus \mathbb{H}_i$. The design of $\mathbb{H}_i(k)$ and $\mathbb{X}_{f,i}$ will be elaborated

in Section 4.1. Finally, the stage cost function $l_i(\bar{x}_i(j|k), \bar{u}_i(j|k), x_i^a(j|k), x_{i,des}(j|k))$ is defined by

$$l_i \triangleq \phi_{i,1}|\bar{\delta}_i(j|k) - \delta_i^a(j|k)| + \phi_{i,2}|\bar{\mathcal{E}}_i(j|k) - \mathcal{E}_i^a(j|k)| + \lambda_{i,1}|\bar{\delta}_i(j|k) - \delta_0| + \lambda_{i,2}|\bar{\mathcal{E}}_i(j|k)_i - \overline{m}_{i,i-1}\mathcal{E}_{i-1}^a(j|k)| \tag{31}$$

where $\phi_{i,1}, \phi_{i,2} \in \mathbb{R}_{>0}$ penalize the differences between the optimal and assumed states and $\lambda_{i,1}, \lambda_{i,2} \in \mathbb{R}_{>0}$ are utilized to penalize the deviation of the optimal states from their desired trajectories. In addition, $\psi_i \in \mathbb{R}_{>0}$ in (26a) is used to ensure the tightness of the inequality condition in (29), thus the validity of the control solution, as will be discussed in Proposition 1.

Overall, the proposed convex and tube-based DMPC algorithm is summarized in Algorithm 1.

Algorithm 1 The local convex and tube-based DMPC algorithm for vehicle $i \in \mathcal{N}$

Offline:

(a) Find the observer and control gains L_i and K_i;
(b) Determine the tightened constraints (26c) and (26d), which are introduced in Section 3.1;
(c) Select suitable weighting parameters $\phi_{i,j}$, $\lambda_{i,j}$, $\psi_i, j = 1, 2$ and the prediction horizon N_p for the $\mathcal{P}_i$ in line with (37) and (44);
(e) Find an initial feasible assumed trajectory $x_i^a(:|0)$.

Online:

while $0 \le k < \bar{k}$ **do**
  Measure the current state $y_i(k)$;
  Obtain the state estimate $\hat{x}_i(k)$ by (15);
  Set the initial condition (26f) of the MPC problem $\mathcal{P}_i(k)$ based on the measured values;
  Receive $x_{i-1}^a(:|k)$ and $u_{i-1}^a(:|k)$ from the preceding vehicle $i-1$;
  if $x_{i-1}^a(N_p|k) = x_{i-1}^a(N_p|k-1)$ **then**
    Solve $\mathcal{P}_i(k)$ with $\hat{\mathcal{E}}_{i-1}(:|k) = \mathcal{E}_{i-1}^a(N_p|k)$
  else if $x_{i-1}^a(N_p|k) \neq x_{i-1}^a(N_p|k-1)$ **then**
    Solve $\mathcal{P}_i(k)$ with $\hat{\mathcal{E}}_{i-1}(:|k) = \mathcal{E}_{i-1}^a(:|k)$
  end if
  Obtain $u_i^*(:|k)$ and $x_i^*(:|k)$;
  Construct $x_i^a(:|k)$ and $u_i^a(:|k)$ by (23)–(25) and send the assumed trajectories to vehicle $i+1$;
  Apply the control action $u_i(k) = u_i^*(0|k) + K_i e_i(k)$ with $e_i(k) = \hat{x}_i(k) - x_i^*(0|k)$ to the actual system (11);
  $k \leftarrow k+1$;
end while

Remark 1. From (27), the construction of $\hat{\mathcal{E}}_{i-1}$ influences $\bar{d}_i$ (via $\bar{d}_{2[1,1]}(k)$) and therefore the design of the tube-based MPC. In particular, $\bar{d}_{i[1,1]}(k)$ denotes the maximum discrepancy between $f_i(\mathcal{E}_{i-1}(k))\Delta s$ and $f_i(\hat{\mathcal{E}}_{i-1}(k))\Delta s$, which is $(\frac{1}{v_{\min}} - \frac{1}{v_{\max}})\frac{\Delta s}{\Delta t_{\max}}$. For instance, considering the parameter choices given in Case study 1 of the Simulation Section (see Table 1 and Table 2), the resulting upper bound of $|d_{i[1,1]}(k)|$ after normalization is 0.033.

4. Theoretical analysis

In this section, recursive feasibility and Lyapunov stability of Algorithm 1 are discussed and rigorously proved under the case that the leading vehicle is driven at a constant speed $v_0(k) = \bar{v}_0, \forall k \ge k_1$.

4.1. Recursive feasibility and legitimacy of the solution

Once the leading vehicle reaches the steady state velocity $\bar{v}_0$, the assumed trajectory of the leading vehicle will also be constant, that is $\mathcal{E}_0^a(:|k) = \overline{m}_{i,0}\mathcal{E}_0$, $\forall k \ge k_1$. According to the first line of (27), the steady state speed of the leading vehicle can be passed on to the ith follower in i steps subject to PF communication topology. Recall the definition of the desired state trajectory employed in each local MPC at the beginning of Section 3.2, it holds that

$$x_{i,des}(j|k) = [\delta_0 \ \overline{m}_{i,0}\mathcal{E}_0]^\top, \forall k \ge k_1 + i, i \in \mathcal{N} \tag{32}$$

Note that the dependence of $x_{i,des}^*(k)$ on k is dropped for clarity since $x_{i,des}^*(k)$ is constant for all $k \ge k_1 + N$. Following assumptions are needed to proceed with the analysis.

Assumption 4.1. All local MPC problems $\mathcal{P}_i(k), \forall i \in \mathcal{N}$ are feasible for $k \le k_1 + N$.

Assumption 4.2. The condition $\mathbb{X}_{f,i} \subseteq \Xi_i$ holds for all $k \ge k_1 + N$ with Ξ_i the one-step predecessor state set, which can be steered to $x_{i,des}(N_p|k)$ by a feasible control action $u_i^a(N_p - 1|k)$ under (26b):

$$\Xi_i \triangleq \{\bar{x}(N_p - 1|k) \mid \exists \bar{u}_i(N_p - 1|k) \text{ fulfills (26d) and (26e)} : \bar{x}(N_p|k) = x_{i,des}(N_p|k)\}.$$

As it can be noticed, the initial feasible assumption in Assumption 4.1 is commonly used in the DMPC framework with unidirectional topologies (Dunbar & Caveney, 2012; Zheng et al., 2016). This can be addressed by a centralized optimization method or by a trial-and-error approach (Farina & Scattolini, 2012) in the distributed fashion, which has been extensively discussed in the literature. Furthermore, Assumption 4.2 characterizes the size of $\bar{\mathbb{U}}_i$ (in terms of the disturbance $\bar{d}_i, \bar{w}_i$) required to ensures that there exists a feasible $u_i^a(N_p - 1|k)$ so that (25) can be achieved. Since $\bar{d}_i$ is a $\mathcal{K}$ function with respect to the radius of the admissible velocity set $\mathcal{V}_{i-1}$ of v_{i-1} (see Remark 1), Assumption 4.2 can be validated for a given platoon system by gradually tightening the admissible velocity set $\mathcal{V}_i$ ($v_i \in \mathcal{V}_i, \forall i \in \{0\} \cup \mathcal{N}$) as $i \to 0$. In other words, ensuring that $\mathcal{V}_{i-1} \subset \mathcal{V}_i, \forall i \in \mathcal{N}$ leads to gradually enlarged admissible control (torque) sets as $i \to N$.

Theorem 4.1. *Under Assumptions 3.1, 4.1 and 4.2, Algorithm 1 is recursively feasible for all followers.*

Proof. Suppose at any step $k > k_1 + N$, there is a solution $(x_i^*(:|k), u_i^*(:|k))$ for $\mathcal{P}_i(k)$ satisfying all constraints (26b)–(26g). In the following, to deal with the coupled state-control constraint (26e), the two control $\bar{u}_i(:|k+1) = [\bar{\zeta}_i(:|k+1) \ \bar{\mathcal{T}}_i(:|k+1)]^\top$ and two state $\bar{x}_i(:|k+1) = [\bar{\delta}_i(:|k+1) \ \bar{\mathcal{E}}_i(:|k+1)]^\top$ sequences will be analyzed separately. Consider a candidate torque sequence constructed by $\bar{\mathcal{T}}_i(:|k+1) = \mathcal{T}_i^a(:|k+1)$ for

Table 1
Heterogeneous vehicle parameters.

Vehicle Index	m_i [kg]	$C_{d,i}$ [N s^2 m^{-2}]	r_i [m]	$T_{i,\min}$ [N m]	$T_{i,\max}$ [N m]
0	1035.7	0.35	0.30	−350	350
1	1178.7	0.37	0.33	−410	410
2	1257.6	0.37	0.33	−450	450
3	1349.1	0.39	0.35	−480	480
4	1434.0	0.41	0.38	−510	510

Table 2
Rest of the parameters.

Description	Symbols	Values
Tire rolling resistance coefficient	C_{f_i}	0.01
Final drive ratio	η_i	3
Gravity constant	g	9.8 N/kg
Predictive Horizon Length	N_p	20
Sampling distance interval	Δs	2 m
Desired time headway	δ_0	1 s
Minimum time headway	$\Delta t_{\min}$	0.5 s
Maximum time headway	$\Delta t_{\max}$	1.5 s

$\mathcal{P}_i(k+1)$. It is immediate to show that $\mathcal{T}_i^a(0:N_p-2|k+1)$ satisfies the constraint (26d), and according to Assumption 4.2, $\mathcal{T}_i^a(N_p-1|k+1)$ is also feasible. Due to the impact of the disturbances $w_i(k+1)$ and $d_i(k+1)$ introduced when $\bar{\mathcal{E}}_i(0|k+1)$ is initialized (see (26f)), the predicted state trajectory $\bar{\mathcal{E}}_i(:|k+1)$ produced by $\mathcal{T}_i^a(:|k+1)$ is different from the assumed state trajectory $\mathcal{E}_i^a(:|k+1)$. Let

$$\varepsilon_1(:|k+1) \triangleq \bar{\mathcal{E}}_i(:|k+1) - \mathcal{E}_i^a(:|k+1).$$

It is clear that

$$\varepsilon_1(j+1|k+1) = a_{i,2}\varepsilon_1(j|k+1),\ \forall j \in \{0,1,\dots,N_p-1\}$$

with $a_{i,2} = A_{i[2,2]}$, which in turn implies

$$\varepsilon_1(j+1|k+1) = a_{i,2}^{j+1}\varepsilon_1(0|k+1),\ j \in \{0,1,\dots,N_p-1\}$$

with $\varepsilon_1(0|k+1) = a_{i,2}w_i(k+1) + d_i(k+1)$. Due to the fact that $|a_{i,2}| < 1$, we have

$$\begin{aligned}|\varepsilon_1(j|k+1)| \ &\le\ |\varepsilon_1(0|k+1)| = |a_{i,2}w_i(k+1) + d_i(k+1)| \\ &\le \bar{w}_i + \bar{d}_i,\ \forall j \in \{0,1,\dots,N_p\}.\end{aligned} \tag{33}$$

Now, we construct

$$\bar{\zeta}_i(j|k+1) = f_i(\bar{\mathcal{E}}_i(j|k+1)),\ \forall j \in \{0,1,\dots,N_p-2\}$$

that follows the equality of (29) to ensure the legitimacy of the candidate solution. Thanks to Assumption 3.1, we have

$$\begin{aligned}|\bar{\zeta}_i(j|k+1) - \zeta_i^a(j|k+1)| \ &=\ |f_i(\bar{\mathcal{E}}_i(j|k+1)) - f_i(\mathcal{E}_i^a(j|k+1))| \\ &\le\ \kappa_i|\bar{\mathcal{E}}_i(j|k+1) - \mathcal{E}_i^a(j|k+1))| \le \kappa_i(\bar{w}_i + \bar{d}_i).\end{aligned}$$

Therefore, the equality condition in (29) holds for $\bar{\zeta}_i(0:N_p-2|k+1)$, while the feasibility of $\zeta_i^a(N_p-1|k+1)$ in terms of (26e) (without ensuring the tightness of (29)) is guaranteed by Assumption 4.2. Let

$$\varepsilon_2(:|k+1) \triangleq \bar{\delta}_i(:|k+1) - \delta_i^a(:|k+1).$$

Then, by following the same steps carried out for $\varepsilon_1(:|k+1)$, it can be shown that for all $j \in \{0,1,\dots,N_p-1\}$, it holds that

$$\varepsilon_2(j+1|k+1) = a_{i,1}\varepsilon_2(j|k+1) + (\bar{\zeta}_i(j|k+1) - \zeta_i^a(j|k+1))\Delta s.$$

As $a_{i,1} = A_{i[1,1]} = 1$, it holds that

$$\begin{aligned}|\varepsilon_2(j+1|k+1)| \ &\le\ a_{i,1}^{j+1}(\bar{w}_i + \bar{d}_i) + \sum_{i=0}^{j} a_{i,1}^{i}\kappa_i(\bar{w}_i + \bar{d}_i)\Delta s \\ &= (\bar{w}_i + \bar{d}_i) + (j+1)\kappa_i(\bar{w}_i + \bar{d}_i)\Delta s \\ &\le (\bar{w}_i + \bar{d}_i) + N_p\kappa_i(\bar{w}_i + \bar{d}_i)\Delta s\end{aligned} \tag{34}$$

In view of (33) and (34), provided that the kth step solution is inside the feasible region $\bar{\mathbb{X}}_i \ominus \mathbb{H}_i(k)$, $\bar{x}_i(:|k+1)$ must be bounded by the enlarged set $\bar{\mathbb{X}}_i \ominus \mathbb{H}_i(k+1)$ with $\mathbb{H}_i(k)$ defined in (28), as required by (26c). Moreover, considering (25), the terminal constraint (26g) of $\bar{x}_i(N_p|k+1)$ is also fulfilled. Therefore, the $(k+1)$ step solution (driven by $\mathcal{T}_i^a(:|k+1)$) is feasible.

The analysis can be applied to all steps $k > k_1 + N$. Hence, it can be concluded by induction that if Assumption 4.1 holds, the proposed algorithm is recursively feasible, and it applies to any vehicle $i \in \mathcal{N}$.

Remark 2. The enlarged set $\mathbb{H}_i$ (see (28)) parameterized by $\bar{k}$ may be too conservative in practice. To reduce the conservativeness, one may set $\mathbb{H}_i(k) = (z-k)\bar{\mathbb{H}}_i$ with $z = k+1, k+2\dots,\bar{k}-1$ and reset the algorithm when the set $\bar{\mathbb{X}}_i \ominus \mathbb{H}_i(k)$ cannot be enlarged any more when $\mathbb{H}_i(k) = \emptyset$. The reset can be performed with reinitialized $\mathbb{H}_i(k) = (z-k)\bar{\mathbb{H}}_i$, $z > k$ from the vehicle where the infeasibility occurs towards the Nth vehicle in a sequential manner.

Theorem 4.1 demonstrates the existence of a feasible and legitimate solution, except for the last step, where the tightness of (29) cannot be guaranteed. However, this does not affect the validity of the closed-loop control solution unless a valid MPC solution (with a guaranteed equality condition of (29)) cannot be found for consecutive N_p steps. In such a case, a sequential reset of the DMPC algorithm will be invoked as with Remark 2. Next, we show that the optimal solution of the finite-horizon optimization problem $\mathcal{P}_i(k)$ tends to find the equality condition of (29).

Given the $(k-1)$th step optimal solution $(x_i^*(:|k-1), u_i^*(:|k-1))$ of $\mathcal{P}_i(k-1)$ and the measurement $y_i(k)$ (which determines the initial condition of $\mathcal{P}_i(k)$), first consider a feasible solutions of $\mathcal{P}_i(k)$, denoted by $(\delta_i^c(:|k), \mathcal{E}_i^c(:|k), \zeta_i^c(:|k), \mathcal{T}_i^c(:|k))$ by which the equality condition $\zeta_i^c(j|k) = f_i(\mathcal{E}_i^c(j|k)),\ \forall j \in \{0,1,\dots,N_p-1\}$ in (29) holds. Then under the same $(x_i^*(:|k-1), u_i^*(:|k-1))$ and $y_i(k)$, it is possible to construct an alternative solution $(\check{\delta}_i(:|k), \check{\mathcal{E}}_i(:|k), \check{\zeta}_i(:|k), \check{\mathcal{T}}_i(:|k))$ with $\check{\delta}_i(0|k) = \delta_i^c(0|k)$, $\check{\mathcal{T}}_i(:|k) = \mathcal{T}_i^c(:|k)$ and $\check{\mathcal{E}}_i(:|k) = \mathcal{E}_i^c(:|k)$ whereas the tightness of (29) does not hold

$$\check{\zeta}_i(j|k) = f_i(\check{\mathcal{E}}_i(j|k)) + \Delta\zeta_i(j|k),\ \ \Delta\zeta_i(j|k) \in \mathbb{R}_{>0}$$

which implies

$$\Delta\zeta_i(j|k) = \check{\zeta}_i(j|k) - \zeta_i^c(j|k),\ \ \forall j \in \{0,1,\dots,N_p-2\}. \tag{35}$$

In view of (11) and (35), the dynamics of δ_i in both scenarios follow

$$\delta_i^c(j+1|k) = \delta_i^c(j|k) + \left(\zeta_i^c(j|k) - f_i\left(\hat{\mathcal{E}}_{i-1}\right)\right)\Delta s \tag{36a}$$

$$\check{\delta}_i(j+1|k) = \check{\delta}_i(j|k) + \left(\zeta_i^c(j|k) + \Delta\zeta_i(j|k) - f_i\left(\hat{\mathcal{E}}_{i-1}\right)\right)\Delta s \tag{36b}$$

The main result is characterized by the following proposition.

Proposition 1. *Given the two feasible solutions* $(\delta_i^c(:|k), \mathcal{E}_i^c(:|k), \zeta_i^c(:|k), \mathcal{T}_i^c(:|k))$ *and* $\left(\check{\delta}_i(:|k), \check{\mathcal{E}}_i(:|k), \check{\zeta}_i(:|k), \check{\mathcal{T}}_i(:|k)\right)$ *defined above, if the weights of the DMPC objective function (31) are chosen such that*

$$\psi_i \ge (N_p-1)\Delta s(\phi_{i,1} + \lambda_{i,1}) \tag{37}$$

the optimal solution of $\mathcal{P}_i(k)$, $\forall k \in \{0,1,\dots,\bar{k}\}$ *always finds* $(\delta_i^c(:|k), \mathcal{E}_i^c(:|k), \zeta_i^c(:|k), \mathcal{T}_i^c(:|k))$ *with guaranteed equality condition of (29).*

Proof. Let $J_i^c(k)$ and $\check{J}_i(k)$ denote the cost in both solution cases. Their difference follows

$$\begin{aligned}&J_i^c(k) - \check{J}_i(k) \\ &= \sum_{j=0}^{N_p-1} l_i\left(x_i^c(j|k), u_i^c(j|k), x_i^a(j|k), x_{i,des}(j|k)\right) + \sum_{j=0}^{N_p-2}\psi_i|\zeta_i^c(j|k) - f_i(\mathcal{E}_i^c(j|k))| \\ &- \left(\sum_{j=0}^{N_p-1} l_i\left(\check{x}_i(j|k), \check{u}_i(j|k), x_i^a(j|k), x_{i,des}(j|k)\right) + \sum_{j=0}^{N_p-2}\psi_i|\check{\zeta}_i(j|k) - f_i(\check{\mathcal{E}}_i(j|k))|\right)\end{aligned} \tag{38}$$

After some rearrangements, we obtain

$$\begin{aligned}J_i^c(k) - \check{J}_i(k) = \sum_{j=0}^{N_p-1}\Big(\ &\phi_{i,1}\left(\ |\delta_i^c(j|k) - \delta_i^a(j|k)| - |\check{\delta}_i(j|k)\right. \\ &\left. - \delta_i^a(j|k)|\ \right) + \lambda_{i,1}\left(|\delta_i^c(j|k) - \delta_0| - |\check{\delta}_i(j|k) - \delta_0|\right)\Big) - \sum_{j=0}^{N_p-2}\psi_i\Delta\zeta_i(j|k)\end{aligned} \tag{39}$$

where the assumed and desired trajectories are identical in both scenarios as they are predefined based on the $(k-1)$th step solution. By the triangle inequality and the identity $\check{\delta}_i(0|k) = \delta_i^c(0|k)$, it holds that

$$\begin{aligned}J_i^c(k) - \check{J}_i(k) \le \sum_{j=1}^{N_p-1}\Big(\ &\phi_{i,1}\left(|\check{\delta}_i(j|k) - \delta_i^c(j|k)|\right) \\ &+ \lambda_{i,1}\left(|\check{\delta}_i(j|k) - \delta_i^c(j|k)|\right)\Big) - \sum_{j=0}^{N_p-2}\psi_i\Delta\zeta_i(j|k)\end{aligned} \tag{40}$$

By subtracting (36a) from (36b), we obtain

$$\check{\delta}_i(j+1|k)-\delta_i^c(j+1|k)=\left(\check{\delta}_i(j|k)-\delta_i^c(j|k)\right)+\Delta\zeta_i(j|k)\Delta s \tag{41}$$

which, by induction, leads to

$$\check{\delta}_i(j+1|k)-\delta_i^c(j+1|k)=\sum_{n=0}^{j}\Delta\zeta_i(n|k)\Delta s. \tag{42}$$

Substituting (42) into (40), it yields

$$\begin{aligned}
&J_i^c(k)-\check{J}_i(k)\\
&\quad\le\sum_{j=1}^{N_p-1}\left(\phi_{i,1}\sum_{n=0}^{j-1}\Delta\zeta_i(n|k)\Delta s+\lambda_{i,1}\sum_{n=0}^{j-1}\Delta\zeta_i(n|k)\Delta s\right)-\psi_i\sum_{j=0}^{N_p-2}\Delta\zeta_i(j|k)\\
&\quad=\Delta s(\phi_{i,1}+\lambda_{i,1})\sum_{j=1}^{N_p-1}\sum_{n=0}^{j-1}\Delta\zeta_i(n|k)-\psi_i\sum_{j=0}^{N_p-2}\Delta\zeta_i(j|k)\\
&\quad\le(N_p-1)\Delta s(\phi_{i,1}+\lambda_{i,1})\sum_{j=0}^{N_p-2}\Delta\zeta_i(j|k)-\psi_i\sum_{j=0}^{N_p-2}\Delta\zeta_i(j|k)
\end{aligned} \tag{43}$$

Given the condition (37), (43) further implies that $J_i^c(k)-\check{J}_i(k)\le 0$, thus ending the proof.

Remark 3. Note that Proposition 1 does not ensure a legitimate solution to be found. The proposed algorithm may still find a solution where the equality condition of (29) is not satisfied within a finite horizon due to the non-strict convexity. In such a case, a legitimate solution (except the last step) can be constructed as a posteriori by following the analysis given in Theorem 4.1. For all the practical scenarios of interest in the present work it has been found that the present formulation yields a tight solution.

4.2. Robustness analysis

Based on Theorem 4.1, this subsection will focus on the Lyapunov stability of the proposed DMPC scheme.

Theorem 4.2. *Under Assumptions 3.1, 4.1 and 4.2, given the Algorithm 1 for $\mathcal{P}_i(k)$, if the weighting parameters are designed such that*

$$\phi_{i,2}\ge\lambda_{i+1,2}\overline{m}_{i+1,i}, \tag{44}$$

the tracking error $x_i(k)-x_{i,des}^*$ of the perturbed system (11) is ISS with respect to the disturbances $d_i(k)$ and $w_i(k)$.

Proof. Without considering the uncertainties $d_i(k)$ and $w_i(k)$, the terminal constraint (26g) of $\mathcal{P}_i(k)$ turns out to $\bar{x}_i(N_p|k)=x_{i,des}(N_p|k)$, which ensures $x_i^*(N_p|k)=x_{i,des}^*$, $\forall k\ge k_1+N$, $i\in\mathcal{N}$. Given $u_i^a(:\,|k+1)$ and $x_i^a(:\,|k+1)$ constructed by (23)–(25), it is straightforward to show they are feasible for $\mathcal{P}_i(k+1)$. In particular, (25) is achieved by employing

$$\begin{aligned}
&\mathcal{T}_i^a(N_p-1|k+1)=\frac{r_i}{\eta_i}\left(\frac{2C_{d,i}}{m_i}(\mathcal{E}_i^a(N_p-1|k+1)+m_igC_{s,i}\right)\\
&\zeta_i^a(N_p-1|k+1)=f_i(\mathcal{E}_i^a(N_p-1|k+1))
\end{aligned}$$

which yields $x_i^a(N_p|k+1)=x_i^a(N_p-1|k+1)=x_i^*(N_p|k)=x_{i,des}^*$. From Theorem 4.1 and Remark 3, $\zeta_i^a(j|k+1)=f_i(\mathcal{E}_i^a(j|k+1))$ holds for all $j\in\{0,1,\dots,N_p-2\}$. By substituting the optimal solution $(x_i^*(:\,|k+1),u_i^*(:\,|k+1))$, the corresponding cost function $J_i^*(k+1)$ can be rewritten as

$$\begin{aligned}
J_i^*(k+1)=&\sum_{j=0}^{N_p-1}\Big(\phi_{i,1}|\delta_i^*(j|k+1)-\delta_i^a(j|k+1)|\\
&+\phi_{i,2}|\mathcal{E}_i^*(j|k+1)-\mathcal{E}_i^a(j|k+1)|+\lambda_{i,1}|\delta_i^*(j|k+1)-\delta_0|\\
&+\lambda_{i,2}|\mathcal{E}_i^*(j|k+1)-\overline{m}_{i,i-1}\mathcal{E}_{i-1}^a(j|k+1)|\Big)\\
\le&\sum_{j=0}^{N_p-1}\Big(\phi_{i,1}|\delta_i^a(j|k+1)-\delta_i^a(j|k+1)|\\
&+\phi_{i,2}|\mathcal{E}_i^a(j|k+1)-\mathcal{E}_i^a(j|k+1)|+\lambda_{i,1}|\delta_i^a(j|k+1)-\delta_0|\\
&+\lambda_{i,2}|\mathcal{E}_i^a(j|k+1)-\overline{m}_{i,i-1}\mathcal{E}_{i-1}^a(j|k+1)|\Big)
\end{aligned} \tag{45}$$

which can be reduced to

$$\begin{aligned}
J_i^*(k+1)\le&\sum_{j=0}^{N_p-1}\Big(\lambda_{i,1}|\delta_i^a(j|k+1)-\delta_0|\\
&+\lambda_{i,2}|\mathcal{E}_i^a(j|k+1)-\overline{m}_{i,i-1}\mathcal{E}_{i-1}^a(j|k+1)|\Big)
\end{aligned} \tag{46}$$

For the sake of further analysis, let us rewrite (46) as

$$\begin{aligned}
J_i^*(k+1)&\le\sum_{j=1}^{N_p}\left(\lambda_{i,1}|\delta_i^*(j|k)-\delta_0|+\lambda_{i,2}|\mathcal{E}_i^*(j|k)-\overline{m}_{i,i-1}\mathcal{E}_{i-1}^*(j|k)|\right)\\
&=\sum_{j=1}^{N_p-1}\left(\lambda_{i,1}|\delta_i^*(j|k)-\delta_0|+\lambda_{i,2}|\mathcal{E}_i^*(j|k)-\overline{m}_{i,i-1}\mathcal{E}_{i-1}^*(j|k)|\right)
\end{aligned} \tag{47}$$

Subtracting $J_i^*(k)$ from $J_i^*(k+1)$,

$$\begin{aligned}
J_i^*(k+1)-J_i^*(k)\le&\\
&-\Big(\phi_{i,1}|\delta_i^*(0|k)-\delta_i^a(0|k)|+\phi_{i,2}|\mathcal{E}_i^*(0|k)-\mathcal{E}_i^a(0|k)|\\
&+\lambda_{i,1}|\delta_i^*(0|k)-\delta_0|+\lambda_{i,2}|\mathcal{E}_i^*(0|k)-\overline{m}_{i,i-1}\mathcal{E}_{i-1}^a(0|k)|\Big)\\
&+\sum_{j=1}^{N_p-1}\left(\lambda_{i,1}|\delta_i^*(j|k)-\delta_0|+\lambda_{i,2}|\mathcal{E}_i^*(j|k)-\overline{m}_{i,i-1}\mathcal{E}_{i-1}^*(j|k)|\right)\\
&-\sum_{j=1}^{N_p-1}\Big(\phi_{i,1}|\delta_i^*(j|k)-\delta_i^a(j|k)|+\phi_{i,2}|\mathcal{E}_i^*(j|k)-\mathcal{E}_i^a(j|k)|\\
&+\lambda_{i,1}|\delta_i^*(j|k)-\delta_0|+\lambda_{i,2}|\mathcal{E}_i^*(j|k)-\overline{m}_{i,i-1}\mathcal{E}_{i-1}^a(j|k)|\Big)
\end{aligned} \tag{48}$$

By applying the triangle inequality, (48) can be reduced to

$$\begin{aligned}
J_i^*(k+1)-J_i^*(k)\le&\\
&-\Big(\phi_{i,1}|\delta_i^*(0|k)-\delta_i^a(0|k)|+\phi_{i,2}|\mathcal{E}_i^*(0|k)-\mathcal{E}_i^a(0|k)|\\
&+\lambda_{i,1}|\delta_i^*(0|k)-\delta_0|+\lambda_{i,2}|\mathcal{E}_i^*(0|k)-\overline{m}_{i,i-1}\mathcal{E}_{i-1}^a(0|k)|\Big)\\
&-\sum_{j=1}^{N_p-1}\Big(\phi_{i,1}|\delta_i^*(j|k)-\delta_i^a(j|k)|+\phi_{i,2}|\mathcal{E}_i^*(j|k)-\mathcal{E}_i^a(j|k)|\\
&-\lambda_{i,2}\overline{m}_{i,i-1}|\mathcal{E}_{i-1}^*(j|k)-\mathcal{E}_{i-1}^a(j|k)|\Big)
\end{aligned} \tag{49}$$

Let us consider the sum of all local cost functions $J_i^*(k)$, $\forall i\in\mathcal{N}$ as a candidate Lyapunov function: $J_\Sigma^*(k)=\sum_{i=1}^N J_i^*(k)$ In view of (49), it can be shown that

$$\begin{aligned}
J_\Sigma^*(k+1)-J_\Sigma^*(k)=&\sum_{i=1}^{N}\left(J_i^*(k+1)-J_i^*(k)\right)\\
\le&-\sum_{i=1}^{N}\Big(\phi_{i,1}|\delta_i^*(0|k)-\delta_i^a(0|k)|+\phi_{i,2}|\mathcal{E}_i^*(0|k)-\mathcal{E}_i^a(0|k)|\\
&+\lambda_{i,1}|\delta_i^*(0|k)-\delta_0|+\lambda_{i,2}|\mathcal{E}_i^*(0|k)-\overline{m}_{i,i-1}\mathcal{E}_{i-1}^a(0|k)|\Big)\\
&-\sum_{i=1}^{N}\sum_{j=1}^{N_p-1}\Big(\phi_{i,1}|\delta_i^*(j|k)-\delta_i^a(j|k)|+\phi_{i,2}|\mathcal{E}_i^*(j|k)-\mathcal{E}_i^a(j|k)|\\
&-\lambda_{i,2}\overline{m}_{i,i-1}|\mathcal{E}_{i-1}^*(j|k)-\mathcal{E}_{i-1}^a(j|k)|\Big)
\end{aligned} \tag{50}$$

Due to the fact that $\lambda_{1,2}\overline{m}_{1,0}|\mathcal{E}_0^*(j|k)-\mathcal{E}_0^a(j|k)|=0$, we have

$$\begin{aligned}
&J_\Sigma^*(k+1)-J_\Sigma^*(k)\\
&\quad\le-\sum_{i=1}^{N}\Big(\phi_{i,1}|\delta_i^*(0|k)-\delta_i^a(0|k)|+\phi_{i,2}|\mathcal{E}_i^*(0|k)-\mathcal{E}_i^a(0|k)|\\
&\quad+\lambda_{i,1}|\delta_i^*(0|k)-\delta_0|+\lambda_{i,2}|\mathcal{E}_i^*(0|k)-\overline{m}_{i,i-1}\mathcal{E}_{i-1}^a(0|k)|\Big)\\
&\quad-\sum_{i=1}^{N}\sum_{j=1}^{N_p-1}\phi_{i,1}|\delta_i^*(j|k)-\delta_i^a(j|k)|-\sum_{j=1}^{N_p}\phi_{N,2}|\mathcal{E}_N^*(j|k)-\mathcal{E}_N^a(j|k)|\\
&\quad-\sum_{i=1}^{N-1}\sum_{j=1}^{N_p-1}(\phi_{i,2}-\lambda_{i,2}\overline{m}_{i,i-1})|\mathcal{E}_i^*(j|k)-\mathcal{E}_i^a(j|k)|
\end{aligned}\tag{51}$$

According to (44), $J_\Sigma^*(k+1)-J_\Sigma^*(k)\le 0$, which further implies the asymptotic convergence of tracking error of each vehicle $\bar{x}_i(k)-x_{i,des}(k), \forall i\in\mathcal{N}$. As the leader information is accessible to Vehicle 1, that is $x_{1,des}=[\delta_0\ \ \overline{m}_{1,0}\mathcal{E}_0(k)]^\top$, it further implies that

$$\bar{x}_i(k)-x_{i,des}^*\to 0, k\to\infty,\ \forall i\in\mathcal{N}.$$

As $x_i(k)-\bar{x}_i(k)=\tilde{x}_i(k)+e_i(k)$ and $\tilde{x}_i(k)$ and $e_i(k)$ are ISS (see (16)–(20)), it is immediate to show that the tracking error $x_i(k)-x_{i,des}^*$ in the presence of disturbances and measurement noise is also ISS and it will converge to a robust invariable set $\bar{\mathbb{S}}_i\oplus\overline{\mathbb{S}}_i$.

Remark 4. The proposed method is based on unidirectional PF topology, which demands less communication compared to other topologies, such as PLF, two predecessor-leader following (TPLF) topologies and other bidirectional counterparts. The proposed control solution can be extended to cope with those graphs (Zheng et al., 2016; Zheng, Li, Wang, Cao, & Li, 2016). If the leader information is immediately available to all followers (*e.g.*, PLF and TPLF), it is usually more straightforward to design a DMPC algorithm by replacing the desired state of the preceding vehicle $\overline{m}_{i,i-1}\mathcal{E}_{i-1}^a(j|k)$ in the local MPC problem (26) with the state $\overline{m}_{i,0}\mathcal{E}_0$ of the leading vehicle.

5. Numerical examples

Two case studies are carried out in this section. In the first case study, a numerical example will first be investigated to show the effectiveness of the proposed algorithm, and then the significance of tube-based DMPC in dealing with system uncertainties by comparing it with the nominal DMPC algorithm. Finally, the proposed method is benchmarked against an existing nominal DMPC-based platooning method (Zheng et al., 2016) in terms of computational efficiency. Case study 2 focuses on a more realistic scenario, where the leader is requested to follow an experimental speed profile. The proposed method demonstrates its ability to maintain platoon formation in this scenario, highlighting its applicability to more practical time-varying velocity scenarios.

In both examples, we consider a vehicle platoon that contains one leading vehicle and four following vehicles. Each individual vehicle exchanges information with its neighbors through a PF communication topology. In Table 1, the parameters of platoon vehicles are given, which reflect the heterogeneity entailed in vehicle mass m_i, air drag coefficient $C_{d,i}$, wheel radius r_i and the driving/braking torque limits $T_{i,\min}$, $T_{i,\max}$. Other common parameters of the vehicle and the DMPC algorithm are included in Table 2. It is noted that a constant tire rolling resistance coefficient, C_{f_i}, is employed as a simple example. This tube-based DMPC problem is solved by Yalmip (Löfberg, 2004) with the convex solver MOSEK (ApS, 2019) in the Matlab environment. The specifications of the PC are Intel Core i5 2.3 GHz CPU with 8 GB of RAM.

5.1. Case study 1

Consider the velocity trajectory of the leading vehicle, as shown in Fig. 2. Assuming the speed limits are set to $v_{\min}=20$ m/s and $v_{\max}=40$ m/s. In addition, the process and measurement disturbances added to the dynamic equations of all followers are subject to $|d_i|\le 0.035$ and $|w_i|\le 0.02,\ \forall i\in\mathcal{N}$. Then, the uncertainty bounds $\bar{d}_i=0.035$ and $\bar{w}_i=0.02, \forall i\in\mathcal{N}$ are exploited for the design of the tube-based DMPC. Finally, the platoon is initialized by the conditions given in Table 3.

Table 3
Vehicle initial conditions in Case study 1.

Vehicle Index	Initial time $t_i(0)$ [s]	Initial Time Headway $\Delta t_i(0)$ [s]	Initial speed $v_i(0)$ [m/s]
0	0	–	23
1	1.1	1.1	23
2	2	0.9	22
3	3.1	1.1	23
4	4	0.9	24

The results are shown in Figs. 2–4, which verify the effectiveness of the proposed control solution. More specifically, the velocity profiles and the resulting tracking error signals are shown in Fig. 2, demonstrated in the time domain for illustrative purposes. Since our control objective (13) is to maintain a constant time headway in the spatial domain, the resulting plots differ from other time domain control methods (Qiang et al., 2022; Zheng et al., 2016) after spatial domain to time domain transformation. The simulation shows that the control signals of all follower vehicles exhibit similar behavior, and therefore for clarity of the figure, only the input torque and the tube of Vehicle 1 are presented in Figs. 3. The chattering behavior primarily results from the uncertainties and may be attenuated by including the dynamics of the torque in the vehicle system model (11). Finally, it can be observed from Fig. 4 that the time headway tracking errors are robustly bounded around the desired values (with no validation against the safety limits) in the presence of the uncertainties.

Then, the proposed tube-based DMPC algorithm is compared with the nominal DMPC in the form of (26) but without the tightening of the feasibility sets (26c) (26d) and the terminal constraint (26g). From Fig. 5, it can be observed that under the same simulation condition shown in Figs. 2 to 4, the time headway trajectory of Vehicle 4 violates the state constraint at the position $s=342$ m, which may cause rear-end collisions in practice. It is noteworthy that the tightening of the feasibility entailed in the tube-based MPC inevitably introduces conservativeness, and may eventually become infeasible when the bound of uncertainty increases. In this context, we also take Vehicle 4 as an example to study the maximum uncertainty that can be tolerant. It is found that the proposed algorithm can tolerate normalized uncertainties up to $\bar{d}_i=0.07$ or $\bar{w}_i=0.07$, which corresponds to a velocity uncertainty of ± 2.8 m/s and a distance headway uncertainty of ± 8.4 m after converting to time domain.

Further simulation is performed to show the computational efficiency of the proposed convex and robust DMPC as compared to Zheng et al. (2016), which proposes a non-convex DMPC algorithm. In order to conduct a fair comparison, we set identical parameters from Table 1 and Table 2. Additionally, the same cost function and weighting coefficients utilized in Zheng et al. (2016) are employed. The computational efficiency of the proposed method is evaluated in Fig. 6 by comparing to a traditional nonlinear DMPC-based method (Zheng et al., 2016) that is solved by IPOPT. As it can be seen, the individual DMPC average running time of each step is 8.5×10^{-3} s. Considering the distance step size and $v_{\max}=40$ m/s, the minimum time duration over a distance step Δs is 0.05 s, which is greater than the computation time and therefore reflects the real-time applicability of the proposed algorithm. In contrast, when the non-convex DMPC algorithm is implemented, the average time consumption of all vehicles is above 0.4 s, considerably more time-consuming compared to the proposed method (approximately 50 times slower on average). The results show the merit of the convex modeling framework.

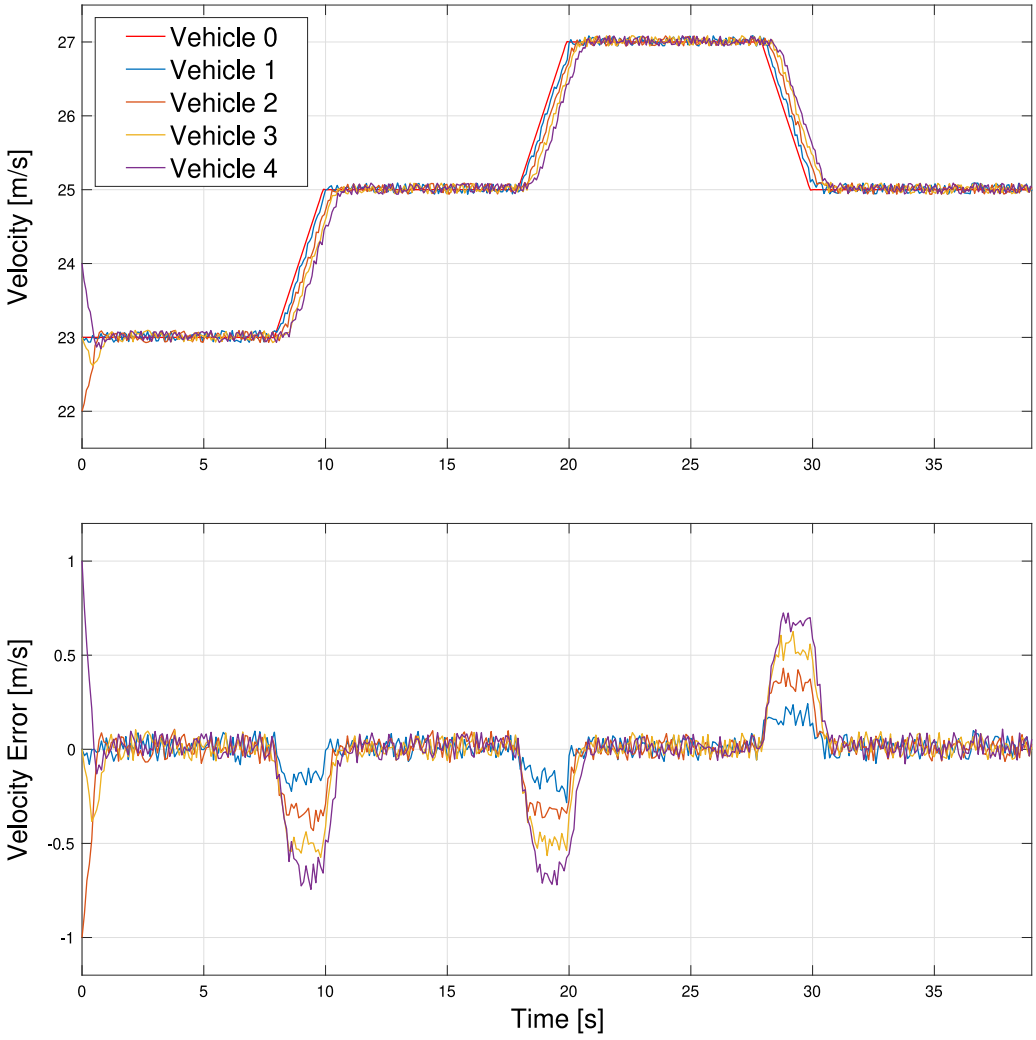

Fig. 2. Top: The velocity performance of all vehicles. Bottom: The velocity tracking performance of all followers.

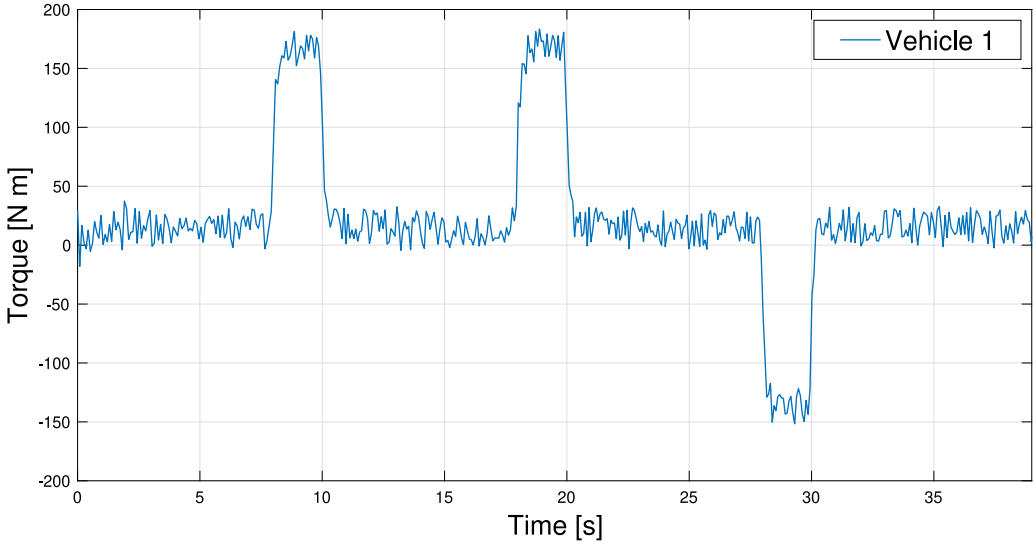

Fig. 3. The input torque of Vehicle 1 in the platoon.

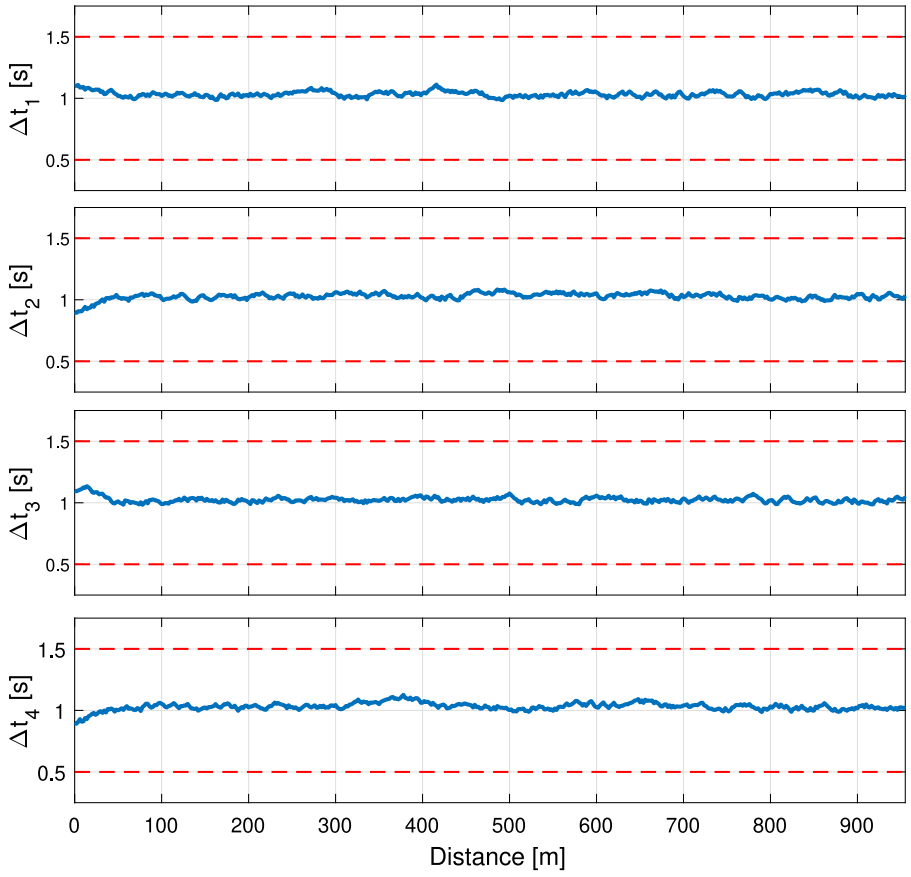

Fig. 4. The time headway profiles of all followers.

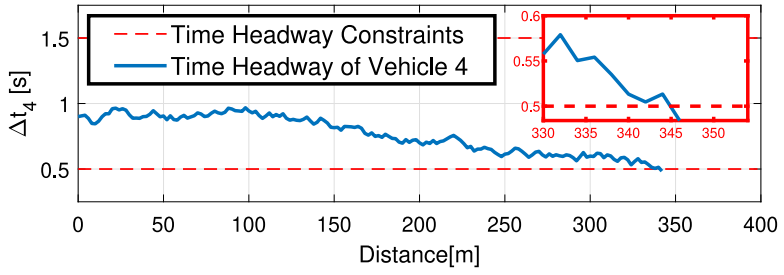

Fig. 5. The time headway of Vehicle 4 obtained by a nominal MPC.

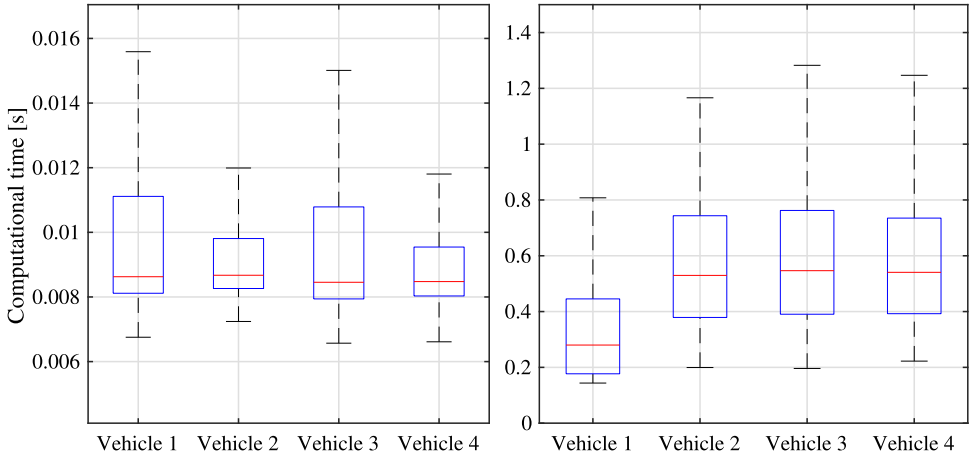

Fig. 6. Left: Computation time of the proposed convex and robust DMPC algorithm. Right: Computation time of the nonlinear DMPC algorithm in Zheng et al. (2016).

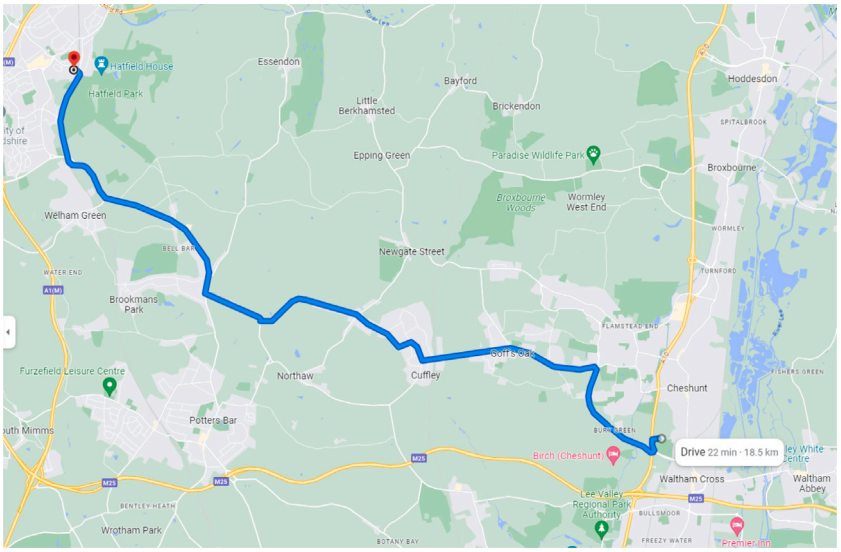

Fig. 7. A 18.5 km rural route in the UK.

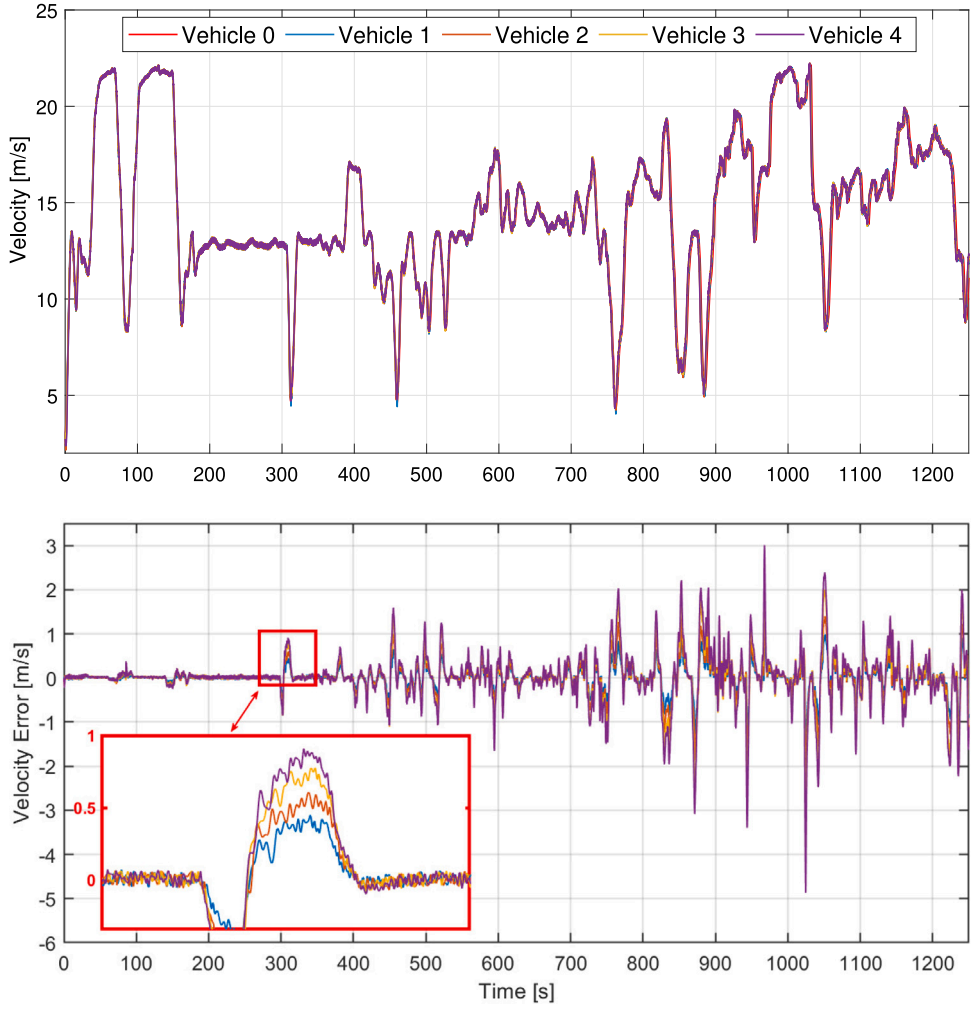

Fig. 8. Top: The velocity performance of all vehicles during rural driving cycles. Bottom: The velocity tracking performance of all followers during the experimental driving profile.

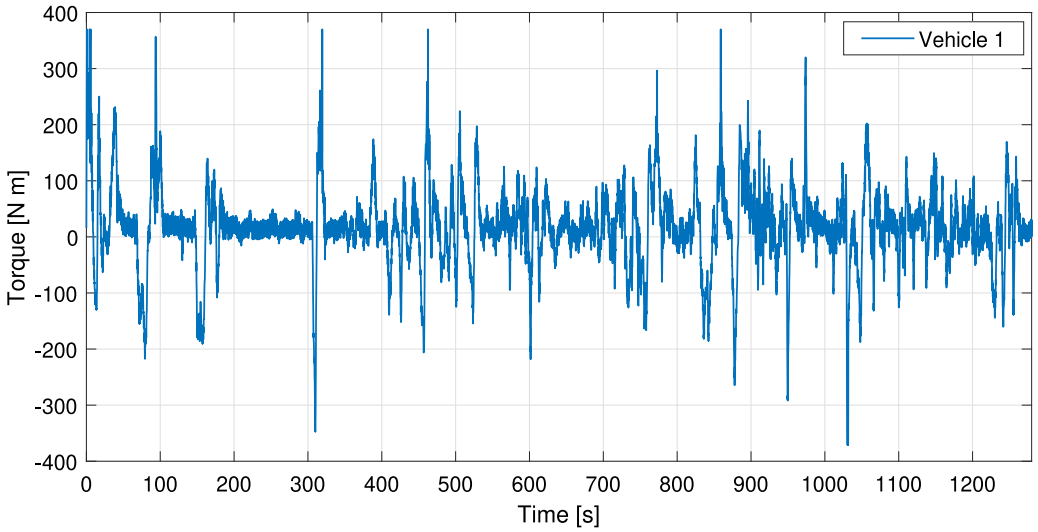

Fig. 9. The input torque of Vehicle 1 during the experimental driving profile.

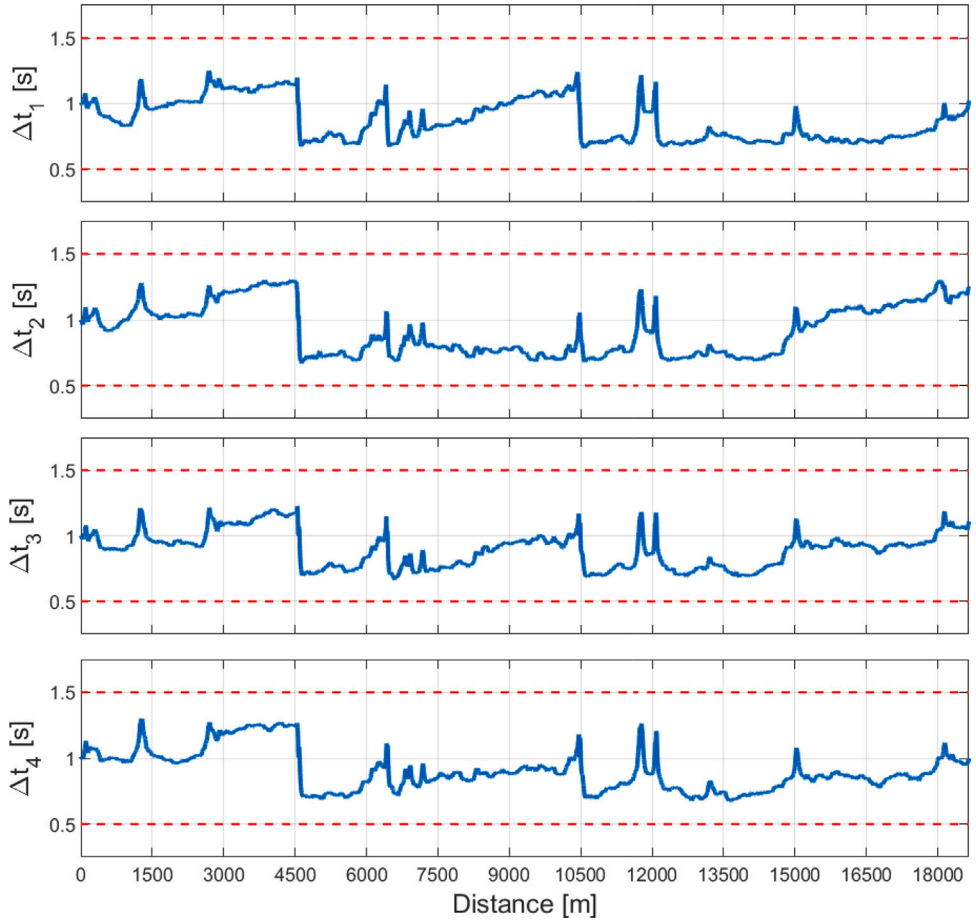

Fig. 10. The time headway profiles during the experimental driving profile.

5.2. Case study 2

In this subsection, we further examine the performance of the proposed method under the condition of continuously changing leader speed, which is taken from an experimental speed profile collected on a rural route in the UK (18.5 km in total, see Fig. 7). The road slope angle $\theta_i(s)$ is collected from Google Maps. The initial conditions of all vehicles are set uniformly as $\Delta t_i(0) = 1$ s and $v_i(0) = 0.91$ m/s for all $i \in \mathcal{N}$.

The velocity tracking performance is illustrated in Fig. 8. The proposed algorithm exhibits highly accurate tracking performance with a maximum error of ± 4.7 m/s throughout the mission. As an example, the torque of Vehicle 1 is plotted in Fig. 9. Similar to Case Study 1, the profile remains noisy despite the respect of the control constraints.

Furthermore, the time headway tracking performance of followers is shown in Fig. 10. Despite the increased complexity of the realistic driving cycle compared to the reference speed profile in Case Study 1, all followers can still maintain their time headway within the safe region with minimal tracking error attributed to system uncertainties.

6. Conclusion

This paper deals with robust vehicle platooning control of heterogeneous CAVs by a convex and tube-based DMPC algorithm, which is able to cope with measurement and modeling uncertainties under PF communication topology. The overall problem is formulated in the space domain rather than using the conventional time domain models, and in this context, the resulting receding horizon optimal control problems can be suitably relaxed as a convex problem, which enables a rapid optimal solution search, which is the key to practical implementation. The relaxation is proved to be valid and non-conservative. The proposed framework also enables coupled state constraints for collision avoidance to be taken into consideration for safety guarantees. Both the recursive feasibility and Lyapunov stability are addressed at the steady state velocity of the leader vehicle. Simulation results verify the effectiveness and robustness of the proposed algorithm, particularly in the presence of an experimental and continuously changing leader speed. Also, by comparing with a benchmark solution in the literature, the proposed algorithm is found to outperform with up to a 50 times improvement in computational efficiency.

Future research efforts will be devoted to the investigation of including more realistic torque dynamics and energy consumption models for smooth and energy-efficient control, and different communication graphs so that the theoretical guarantees can be justified for all steps. Moreover, we will extend the control framework to incorporate communication delays and platoon reconfiguration as well as interactions with human-driven vehicles.

CRediT authorship contribution statement

Hao Sun: Conceptualization, Methodology, Software, Writing – original draft. **Li Dai:** Formal analysis, Methodology, Writing – review & editing. **Giuseppe Fedele:** Formal analysis, Validation. **Boli Chen:** Resources, Supervision, Writing – review & editing, Funding acquisition, Project administration.

Declaration of competing interest

The authors declare that they have no known competing financial interests or personal relationships that could have appeared to influence the work reported in this paper.

Acknowledgments

This work has been supported by The Royal Society Grant, UK, IES\R2\212041.

References

An, G., & Talebpour, A. (2023). Vehicle platooning for merge coordination in a connected driving environment: A hybrid ACC-DMPC approach. *IEEE Transactions on Intelligent Transportation Systems*, *24*(5), 5239–5248.

ApS, M. (2019). The MOSEK optimization toolbox for MATLAB manual. Version 9.0..

Boo, J., & Chwa, D. (2023). Integral sliding mode control-based robust bidirectional platoon control of vehicles with the unknown acceleration and mismatched disturbance. *IEEE Transactions on Intelligent Transportation Systems*.

Dunbar, W. B., & Caveney, D. S. (2012). Distributed receding horizon control of vehicle platoons: Stability and string stability. *IEEE Transactions Automatic Control*, *57*(3), 620–633.

Farina, M., & Scattolini, R. (2012). Distributed predictive control: A non-cooperative algorithm with neighbor-to-neighbor communication for linear systems. *Automatica*, *48*(6), 1088–1096.

Feng, S., Song, Z., Li, Z., Zhang, Y., & Li, L. (2021). Robust platoon control in mixed traffic flow based on tube model predictive control. *IEEE Transactions on Intelligent Vehicles*, *6*(4), 711–722.

Feng, S., Zhang, Y., Li, S. E., Cao, Z., Liu, H. X., & Li, L. (2019). String stability for vehicular platoon control: Definitions and analysis methods. *Annual Reviews in Control*, *47*, 81–97.

Gong, S., & Du, L. (2018). Cooperative platoon control for a mixed traffic flow including human drive vehicles and connected and autonomous vehicles. *Transportation Research Part B: Methodological*, *116*, 25–61.

Gungor, O. E., & Al-Qadi, I. L. (2020). All for one: Centralized optimization of truck platoons to improve roadway infrastructure sustainability. *Transportation Research Part C (Emerging Technologies)*, *114*, 84–98.

Guo, J., Guo, H., Liu, J., Cao, D., & Chen, H. (2022). Distributed data-driven predictive control for hybrid connected vehicle platoons with guaranteed robustness and string stability. *IEEE Internet of Things Journal*, *9*(17), 16308–16321.

Hu, J., Bhowmick, P., Arvin, F., Lanzon, A., & Lennox, B. (2020). Cooperative control of heterogeneous connected vehicle platoons: An adaptive leader-following approach. *IEEE Robotics and Automation Letters*, *5*(2), 977–984.

Huang, Z., Chu, D., Wu, C., & He, Y. (2019). Path planning and cooperative control for automated vehicle platoon using hybrid automata. *IEEE Transactions on Intelligent Transportation Systems*, *20*(3), 959–974.

Kanafani, A., & Parsons, R. (1989). Program on advanced technology for the highway: vehicle/highway research and development. In *Conference record of papers presented at the first vehicle navigation and information systems conference* (pp. 270–272).

Karafyllis, I., Theodosis, D., & Papageorgiou, M. (2023). Nonlinear adaptive cruise control of vehicular platoons. *International Journal of Control*, *96*(1), 147–169.

Lan, J., Zhao, D., & Tian, D. (2021). Data-driven robust predictive control for mixed vehicle platoons using noisy measurement. *IEEE Transactions on Intelligent Transportation Systems*, *24*(6), 6586–6596.

Li, K., Bian, Y., Li, S. E., Xu, B., & Wang, J. (2020). Distributed model predictive control of multi-vehicle systems with switching communication topologies. *Transportation Research Part C (Emerging Technologies)*, *118*, Article 102717.

Li, S., Li, K., Rajamani, R., & Wang, J. (2011). Model predictive multi-objective vehicular adaptive cruise control. *IEEE Transactions on Control Systems Technology*, *19*(3), 556–566.

Liu, P., Kurt, A., & Ozguner, U. (2019). Distributed model predictive control for cooperative and flexible vehicle platooning. *IEEE Transactions on Control Systems Technology*, *27*(3), 1115–1128.

Liu, Y., Xu, L., Cai, G., Yin, G., & Yan, F. (2023). Distributed robust platooning control for heterogeneous vehicle group under parametric uncertainty and hybrid attacks. *IEEE Transactions on Vehicular Technology*.

Liu, Y., Yao, D., Wang, L., & Lu, S. (2022). Distributed adaptive fixed-time robust platoon control for fully heterogeneous vehicles. *IEEE Transactions on Systems, Man, and Cybernetics: Systems*, *53*(1), 264–274.

Löfberg, J. (2004). YALMIP : A toolbox for modeling and optimization in MATLAB. In *Proc. of the CACSD conference*. Taipei, Taiwan.

Lunze, J. (2019). Adaptive cruise control with guaranteed collision avoidance. *IEEE Transactions on Intelligent Transportation Systems*, *20*(5), 1897–1907.

Luo, Q., Nguyen, A.-T., Fleming, J., & Zhang, H. (2021). Unknown input observer based approach for distributed tube-based model predictive control of heterogeneous vehicle platoons. *IEEE Transactions on Vehicular Technology*, *70*(4), 2930–2944.

Mayne, D. Q., Raković, S. V., Findeisen, R., & Allgöwer, F. (2006). Robust output feedback model predictive control of constrained linear systems. *Automatica*, *42*(7), 1217–1222.

Ozkan, M. F., & Ma, Y. (2022). Distributed stochastic model predictive control for human-leading heavy-duty truck platoon. *IEEE Transactions on Intelligent Transportation Systems*, 1–13.

Pi, D., Xue, P., Xie, B., Wang, H., Tang, X., & Hu, X. (2022). A platoon control method based on DMPC for connected energy-saving electric vehicles. *IEEE Transactions on Transportation Electrification*, *8*(3), 3219–3235.

Qiang, Z., Dai, L., Chen, B., & Xia, Y. (2022). Distributed model predictive control for heterogeneous vehicle platoon with inter-vehicular spacing constraints. *IEEE Transactions on Intelligent Transportation Systems*, *24*(3), 3339–3351.

Robinson, T., Chan, E., & Coelingh, E. (2010). Operating platoons on public motorways: An introduction to the sartre platooning programme. In *17th world congress on intelligent transport systems*: *vol. 1*, (p. 12).

Seiler, P., Pant, A., & Hedrick, K. (2004). Disturbance propagation in vehicle strings. *IEEE Transactions on Automatic Control*, *49*(10), 1835–1841.

Shladover, S., Desoer, C., Hedrick, J., Tomizuka, M., Walrand, J., Zhang, W.-B., et al. (1991). Automated vehicle control developments in the PATH program. *IEEE Transactions on Vehicular Technology*, *40*(1), 114–130.

Stankovic, S., Stanojevic, M., & Siljak, D. (2000). Decentralized overlapping control of a platoon of vehicles. *IEEE Transactions on Control Systems Technology*, *8*(5), 816–832.

Sun, H., Dai, L., & Chen, B. (2022). Tube-based distributed model predictive control for heterogeneous vehicle platoons via convex optimization. In *2022 IEEE 25th international conference on intelligent transportation systems* (pp. 1122–1127). IEEE.

Tsugawa, S. (2013). An overview on an automated truck platoon within the energy ITS project. *IFAC Proceedings Volumes*, *46*(21), 41–46.

Turri, V., Besselink, B., & Johansson, K. H. (2017). Cooperative look-ahead control for fuel-efficient and safe heavy-duty vehicle platooning. *IEEE Transactions on Control Systems Technology*, *25*(1), 12–28.

Vilaivannaporn, W., Boonsith, S., Pornputtapitak, W., & Bumroongsri, P. (2021). Robust output feedback predictive controller with adaptive invariant tubes and observer gains. *International Journal of Dynamics and Control*, *9*(2), 755–765.

Wang, P., Deng, H., Zhang, J., Wang, L., Zhang, M., & Li, Y. (2021). Model predictive control for connected vehicle platoon under switching communication topology. *IEEE Transactions on Intelligent Transportation Systems*, 1–14.

Wang, Z., Gao, Y., Fang, C., Liu, L., Zhou, H., & Zhang, H. (2020). Optimal control design for connected cruise control with stochastic communication delays. *IEEE Transactions on Vehicular Technology*, *69*(12), 15357–15369.

Wang, H., Peng, L.-M., Wei, Z., Yang, K., Bai, X.-X., Jiang, L., et al. (2023). A holistic robust motion control framework for autonomous platooning. *IEEE Transactions on Vehicular Technology*.

Xu, L., Jin, X., Wang, Y., Liu, Y., Zhuang, W., & Yin, G. (2022). Stochastic stable control of vehicular platoon time-delay system subject to random switching topologies and disturbances. *IEEE Transactions on Vehicular Technology*, *71*(6), 5755–5769.

Yu, K., Yang, H., Tan, X., Kawabe, T., Guo, Y., Liang, Q., et al. (2016). Model predictive control for hybrid electric vehicle platooning using slope information. *IEEE Transactions on Intelligent Transportation Systems*, *17*(7), 1894–1909.

Zheng, Y., Li, S. E., Li, K., Borrelli, F., & Hedrick, J. K. (2016). Distributed model predictive control for heterogeneous vehicle platoons under unidirectional topologies. *IEEE Transactions on Control Systems Technology*, *25*(3), 899–910.

Zheng, Y., Li, S. E., Wang, J., Cao, D., & Li, K. (2016). Stability and scalability of homogeneous vehicular platoon: Study on the influence of information flow topologies. *IEEE Transactions on Intelligent Transportation Systems*, *17*(1), 14–27.

Zhou, J., Tian, D., Sheng, Z., Duan, X., Qu, G., Cao, D., et al. (2022a). Decentralized robust control for vehicle platooning subject to uncertain disturbances via super-twisting second-order sliding-mode observer technique. *IEEE Transactions on Vehicular Technology*, *71*(7), 7186–7201.

Zhou, J., Tian, D., Sheng, Z., Duan, X., Qu, G., Zhao, D., et al. (2022b). Robust min-max model predictive vehicle platooning with causal disturbance feedback. *IEEE Transactions on Intelligent Transportation Systems*, *23*(9), 15878–15897.

Zhu, Y., Zhao, D., & Zhong, Z. (2019). Adaptive optimal control of heterogeneous CACC system with uncertain dynamics. *IEEE Transactions on Control Systems Technology*, *27*(4), 1772–1779.